



**US Army Corps
of Engineers®**
Engineer Research and
Development Center



DoD Corrosion Prevention and Control Program

Demonstration of Corrosion-Resistant Hybrid Composite Bridge Beams for Structural Applications

Final Report on Project F12-AR15

Steven C. Sweeney, Richard G. Lampo, James Wilcoski,
Chris Olaes, and Larry Clark

September 2016



The U.S. Army Engineer Research and Development Center (ERDC) solves the nation's toughest engineering and environmental challenges. ERDC develops innovative solutions in civil and military engineering, geospatial sciences, water resources, and environmental sciences for the Army, the Department of Defense, civilian agencies, and our nation's public good. Find out more at www.erdclibrary.usace.army.mil.

To search for other technical reports published by ERDC, visit the ERDC online library at <http://acwc.sdp.sirsi.net/client/default>.

Demonstration of Corrosion-Resistant Hybrid Composite Bridge Beams for Structural Applications

Final Report on Project F12-AR15

Steven C. Sweeney, Richard G. Lampo, and James Wilcoski

*Construction Engineering Research Laboratory
U.S. Army Engineer Research and Development Center
2902 Newmark Drive
Champaign, IL 61822*

Christopher Olaes and Larry Clark

*Mandaree Enterprise Corporation
812 Park Drive
Warner Robins, GA 31088*

Final report

Approved for public release; distribution is unlimited.

Prepared for Office of the Secretary of Defense (OUSD(AT&L))
Washington, DC 20301-3090

Under Project F12-AR15, "Corrosion-Resistant Hybrid Composite Bridge Beams for
Structural Applications"

Abstract

The Army has 1,500 vehicular bridges on its installations that can incur high maintenance costs and even early replacement as a result of corrosion of the steel support structures or the reinforcing bar in the concrete. The application of corrosion-resistant technology can extend the service life of bridges and reduce maintenance costs. The Office of the Secretary of Defense Corrosion Prevention and Control Program project demonstrated and validated a corrosion-resistant hybrid-composite beam (HCB) for the reconstruction of a one span of a traditional steel and concrete bridge at Fort Knox, Kentucky. The HCBs were installed on half of the bridge, and conventional steel beams were installed on the other half. Structural analysis of the bridge was performed, and the span with HCBs was found to meet all design specifications and load ratings. This technology can increase the life cycle of bridge infrastructure when utilized in new construction and replacement by the Army and all other federal agencies. The technology's return on investment (ROI) is 4.22.

DISCLAIMER: The contents of this report are not to be used for advertising, publication, or promotional purposes. Citation of trade names does not constitute an official endorsement or approval of the use of such commercial products. All product names and trademarks cited are the property of their respective owners. The findings of this report are not to be construed as an official Department of the Army position unless so designated by other authorized documents.

DESTROY THIS REPORT WHEN NO LONGER NEEDED. DO NOT RETURN IT TO THE ORIGINATOR.

Contents

Abstract	ii
Figures and Tables	iv
Preface	vi
Unit Conversion Factors	vii
1 Introduction	1
1.1 Problem statement.....	1
1.2 Objective.....	3
1.3 Approach.....	3
1.4 Metrics.....	3
2 Technical Investigation	5
2.1 Technology description.....	5
2.2 Field work.....	9
2.3 Commissioning and monitoring.....	15
3 Discussion	18
3.1 Results.....	18
3.1.1 Site corrosivity.....	18
3.1.2 Load testing.....	19
3.2 Lessons learned.....	23
4 Economic Summary	25
4.1 Costs and assumptions.....	25
4.2 Projected return on investment (ROI).....	26
5 Conclusions and Recommendations	28
5.1 Conclusions.....	28
5.2 Recommendations.....	29
5.2.1 Applicability.....	29
5.2.2 Implementation.....	29
References	30
Appendix A: Engineering Drawings for Bridge No. 4, Fort Knox, Kentucky	33
Appendix B: Corrosion Potential Assessment for Bridge No. 4, Fort Knox, Kentucky	42
Appendix C: Excerpts from Hybrid-Composite Beam (HCB®) Design and Maintenance Manual	69
Report Documentation Page	

Figures and Tables

Figures

Figure 1. Bridge No. 4 at Fort Knox.....	2
Figure 2. Composite beam components.	7
Figure 3. Ports for injecting SCC.	7
Figure 4. Interior view of a concrete-filled HCB.....	8
Figure 5. Cross section geometry of a typical HCB.	8
Figure 6. Corroded support beam structure visible during demolition.	10
Figure 7. Lifting degraded steel beam structure during demolition.	10
Figure 8. HCB as delivered to site.	11
Figure 9. Slump test of SCC.....	11
Figure 10. Casting the internal compression reinforcement arch.	12
Figure 11. Span of Bridge No. 4 (foreground) prior to installing HCBs.....	12
Figure 12. Crane lifting an HCB for installation.	13
Figure 13. Placing an HCB.....	13
Figure 14. Forming bridge deck and installing rebar.	14
Figure 15. Bridge deck construction in progress.	14
Figure 16. Completed bridge No. 4 with HCBs (left) and Gridform deck on Cor Ten® weathering steel beams (right).....	15
Figure 17. Weighing a truck to be used for load testing.	16
Figure 18. Two-lane load testing.....	16

Tables

Table 1. Summary of weather data collected December 2012 – December 2013.	18
Table 2. Summary of results from the 6-month ASTM G1 mass loss test and corrosion classification per ISO 9223:2012.....	18
Table 3. Summary of results from the 12-month ASTM G1 mass loss test and corrosion classification per ISO 9223:2012.....	19
Table 4. Atmospheric corrosion severity classification from weather data and ISO 9223:2012 response equation calculations.....	19
Table 5. Controlling rating factors and responses—girders in shear (MEC).....	21
Table 6. Strength rating factors and responses—HCBs in positive flexure (Table 4.5 in Commander and Carpenter 2016).	21
Table 7. Controlling tonnage rating factors for all military loads (Table 4.8 in Commander and Carpenter 2016).....	22
Table 8. Controlling strength rating factors and responses—HCBs in shear limited by GFRP shells (Table 4.7 in Commander and Carpenter 2016).....	22
Table 9. Controlling tonnage rating factors for all military loads (Table 4.8 in Commander and Carpenter 2016).....	23

Table 10. Breakdown of total project costs.....25
Table 11. Project field monitoring costs.25
Table 12. Return on investment calculation.27

Preface

This demonstration was performed for the Office of the Secretary of Defense (OSD) under Department of Defense (DoD) Corrosion Control and Prevention Project F12-AR15, “Corrosion-Resistant Hybrid Composite Bridge Beams for Structural Applications.” The proponent was the U.S. Army Office of the Assistant Chief of Staff for Installation Management (ACSIM), and the stakeholder was the U.S. Army Installation Management Command (IMCOM). The technical monitors were Daniel J. Dunmire (OUSD(AT&L)), Bernie Rodriguez (IMPW-FM), and Valerie D. Hines (DAIM-ODF).

The work was performed by the Materials and Structures Branch of the Facilities Division (CEERD-CF-M), U.S. Army Engineer Research and Development Center, Construction Engineering Research Laboratory (ERDC-CERL). A portion of this work was performed by Christopher Olaes and Larry Clark of Mandaree Enterprise Corp. (MEC), Warner Robins, GA. At the time this report was prepared, Vicki L. Van Blaricum was Chief, CEERD-CFM; Donald K Hicks was Chief, CEERD-CF; and Kurt Kinnevan, CEERD-CZT, was the Technical Director for Adaptive and Resilient Installations. The Deputy Director of ERDC-CERL was Dr. Kirankumar Topudurti and the Director was Dr. Ilker Adiguzel.

The outstanding contributions of subcontractor Brett Commander, Bridge Diagnostics, Inc., who performed the load testing and analysis are gratefully acknowledged.

The following personnel are also gratefully acknowledged for their support and assistance in this project:

- Leo Schmidt – Directorate of Public Works, Fort Knox, KY
- John Wiseman – Directorate of Public Works, Fort Knox, KY
- Rodney Mason – Installation Range Control Officer, Fort Knox, KY
- Butch Faust – All Cities Enterprises, Fort Knox, KY

The Commander of ERDC was COL Bryan S. Green and the Director was Dr. Jeffery P. Holland.

Unit Conversion Factors

Multiply	By	To Obtain
feet	0.3048	meters
gallons (U.S. liquid)	3.785412 E-03	cubic meters
inches	0.0254	meters
mils	0.0254	millimeters
pounds (force)	4.448222	newtons
tons (2,000 pounds, mass)	907.1847	kilograms

(This page intentionally blank.)

1 Introduction

1.1 Problem statement

The Army has installations around the world, and many of these have bridges as a significant part of their infrastructure. These bridges, like those in our national highway system, are experiencing significant deterioration from corrosion of the steel structure and/or the steel reinforcement bars in the concrete. Federal Highway Administration (FHWA) Report RD-01-156 states that approximately one-quarter of the direct cost of corrosion of bridges is made up of maintenance and capital costs for steel reinforcement (Koch et al. 2002). Maintaining serviceable bridges is essential to providing access to the facilities on the post and to remote training areas that would otherwise be inaccessible due to rivers, streams, trains, roads, and other geographical obstacles to transportation. Thus the cost for maintenance and replacement of bridge infrastructure has a big impact on the Army and its operations.

The current technology employed in bridge infrastructure typically has a 50-year design life; however, according to the Illinois and New York state departments of transportation—two states where road salts are used extensively for deicing—the average service life of a steel-reinforced concrete bridge deck is 25 years (Hastak, Halpin, and Hong 2004). The inventory for the Army's bridge safety program shows that more than 80% of its bridges employ standard steel, concrete, or steel and concrete construction (Dean 2008). Bridges are exposed to all climate conditions and often are exposed to heavy industrial contaminants as well. Both design and construction experience show that this exposure is currently an added problem for corrosion because it results in cracking and spalling of concrete beams and corrosion of steel beams. In addition, bridges located in northern regions are frequently exposed to deicing salts in winter weather, and in coastal areas, they are exposed to splash-zone seawater—both conditions accelerate corrosion problems.

New technologies employing corrosion-resistant composite materials are still under development and evaluation as replacements for steel and concrete. The validation and implementation of these technologies will allow DoD installations to utilize them for replacing or rehabilitating corroding

bridge structures. Use of the new technologies could reduce maintenance costs, sustain the mission, and prevent premature failure of infrastructure.

This Corrosion Prevention and Control (CPC)-funded project was a collaboration between the Engineer Research and Development Center–Construction Engineering Research Laboratory (ERDC-CERL) and the Fort Knox Directorate of Public Works (DPW). The Fort Knox DPW has an ongoing initiative to replace or rehabilitate bridges that are severely corroded throughout the installation’s vast training range. Fort Knox is a training base for the Army’s mobile armor combat, and its bridges must carry some of the Army’s heaviest vehicles. These vehicles include the M1A1 Abrams Battle Tank, M2A3 Bradley, and Heavy Equipment Transporter (HET). When carrying the M1A1, a HET has a combined weight of at least 105 tons. The HETS and M1A1 were used in the second load test of the bridge to validate the ability of the HCBs to perform to these demanding requirements.

Bridge No. 4 (Figure 1) in the Fort Knox training range was one of the bridges scheduled for rehabilitation of its corroded support beams and deteriorating bridge deck. With Bridge No. 4 having two spans, it was an excellent candidate for concurrent demonstrations of the HCB and composite deck technologies.

Figure 1. Bridge No. 4 at Fort Knox.



1.2 Objective

The objective of this project was to demonstrate and validate the capabilities of hybrid composite bridge beams as replacements for either conventional concrete or steel beams.

1.3 Approach

The selected demonstration structure was Bridge No. 4, a two-span bridge on the training range at Fort Knox where the support beams and bridge deck were scheduled for replacement due to corrosion damage. This bridge served as the site for two separately funded but concurrent CPC projects—the one documented in this report and CPC Project F12-AR01, which is documented in ERDC/CERL TR-16-21 (Sweeney et al. 2016). The demonstration documented here involves the use of Hillman Composite Beams (HCBs)¹ on one span of the bridge to support a standard steel-reinforced concrete deck. The other span of the bridge (used in Project F12-AR01) demonstrated a composite-grid concrete-reinforcement deck system that is supported by conventional steel beams.

1.4 Metrics

The corrosion potential of the site was determined by using the combination of exposed atmospheric coupons, collected weather data, and corrosion sensors embedded in the new concrete deck. The atmospheric coupon rack was built and tested in accordance with ASTM G1-03, “Standard Practice for Preparing, Cleaning and Evaluating Corrosion Test Specimens,” with the exception of the silver coupons. The silver coupons were tested in accordance with ASTM B825-02, “Standard Test Method for Coulometric Reduction of Surface Films on Metallic Tests.” The results from testing the atmospheric coupons and the collected weather data were analyzed using ISO 9223:2012, “Corrosion of Metal and Alloys – Corrosivity of Atmospheres – Classification, Determination and Estimation.” A summary of the results of the corrosion potential assessment for Bridge No. 4 is shown in section 3.1.1. Details of the corrosion potential analysis are presented in Appendix B of this report.

¹ Hillman Composite Beam and HCB are now registered trademarks of Hillman Inc. of Alpharetta, Georgia. HCB originally was used by Hillman, Inc. to mean “hybrid composite beam,” which is how it is being used in this report.

The design and materials of the HCBs were assessed for corrosion resistance and for meeting design specifications and strength. Structural evaluation was achieved through structural load testing and load rating of the completed structure immediately after construction and again one year after construction. Corrosion was assessed by accumulating data from sensors. Further details of the assessments, done under contract by Bridge Diagnostics Inc. of Boulder, Colorado, are contained in ERDC/CERL CR-16-5 (Commander and Crider 2016).

2 Technical Investigation

2.1 Technology description

The HCB is fabricated from a variety of materials and has a distinctive, specialized configuration. All materials are corrosion resistant, and the fully formed beam weighs much less than conventional steel beams or concrete reinforced beams. The HCB consists of a glass fiber reinforced plastic (GFRP) shell, tension reinforcement stainless steel cables, low-density foam core, and a concrete arch that provides compression reinforcement (Figure 2). The manufacturing process uses vacuum-assisted resin transfer molding (VARTM) technology, which allows for customization of dimensions, shape, and internal lay-up.

The beam's shell is made of vinyl ester resin that is reinforced by glass fibers to resist the design forces. The shell consists of a top flange, a bottom flange, and a continuous conduit. The conduit runs longitudinally and continuously between the ends of the beam and along an arch profile that functions as the internal load path that resists external forces applied to the beam. The HCB is designed to resist the compression and shear forces from loads on the bridge by using the profile of the concrete arch to create compression reinforcement. The arch is fabricated by pumping self-consolidating concrete (SCC) through ports located in the centerline of the beam (Figure 3). Additional ports may be added at 15- to 20-foot spacing, depending on the lengths of the beams.

As can be seen in Figure 2, the cross section of the HCB has significantly less concrete than a standard concrete beam, with some concrete being replaced by lightweight foam. Since the HCB is normally shipped and erected before being filled with concrete, the weight of the HCB is 10% that of a conventional concrete beam and 33% that of a steel beam for typical 70-foot spans (HC Bridge Company, LLC n.d.). Lighter weights mean that transportation costs are less, and beam placement can be accomplished with much smaller cranes, achieving another cost reduction. Even after filling (Figure 4), the HCB is 33% of the weight of a concrete beam and roughly the same weight of a steel beam for typical 70 foot spans (HC Bridge Company, LLC n.d.).

The bridge loads exert thrust on the compression reinforcement and this thrust is resisted and equilibrium maintained by the tension reinforcement located in the bottom of the HCB. This tension reinforcement is comprised of layers of unidirectional steel reinforcing fibers (usually 2,370 ksi, galvanized, prestressing strand) with a high tensile strength and high elastic modulus. These fibers are in the bottom of the HCB and are encapsulated in the FRP during fabrication of the beam shell (Hillman 2012, 2). There are two vertical webs in the beam shell (Figure 5) that transfer applied loads to the composite beam and transfer shear forces between the compression reinforcement and tension reinforcement. The beam shell components are all fabricated monolithically using the VARTM process.

To create compression reinforcement requires that SCC be poured into the HCB shell. This operation can be done at different stages depending on the requirements of a particular installation. The SCC can be placed into the HCB shell prior to shipping the HCB, at the bridge site prior to installing the HCB, or after the HCB shell has been placed on the bridge. These options offer flexibility during the construction process. The only significant variable is that when the HCB is precast before placement on the bridge, the pick points for lifting must be at the ends of the beam so the HCB can carry the added weight of the SCC. When the beam is precast, lifting loops are inserted in the ports for filling the beam with the SCC to provide lift points (visible as loops at the top of the beam in Figure 3). The HCB empty shell can be picked up from any of these lift points on the beam.

A specific HCB design is developed for each individual bridge application based on engineering requirements for the span and allowed loads. The HCBs used for Bridge No. 4 were designed to meet the load requirements in the bridge engineering drawings shown in Appendix A. Constructing a bridge using HCBs is accomplished in the same way as using steel beams or prestressed concrete beams.

Figure 2. Composite beam components.

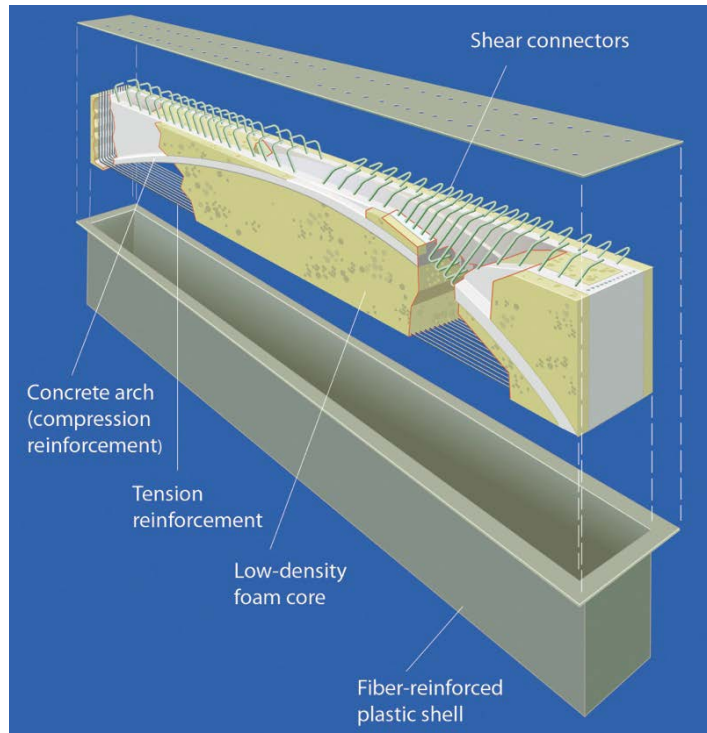


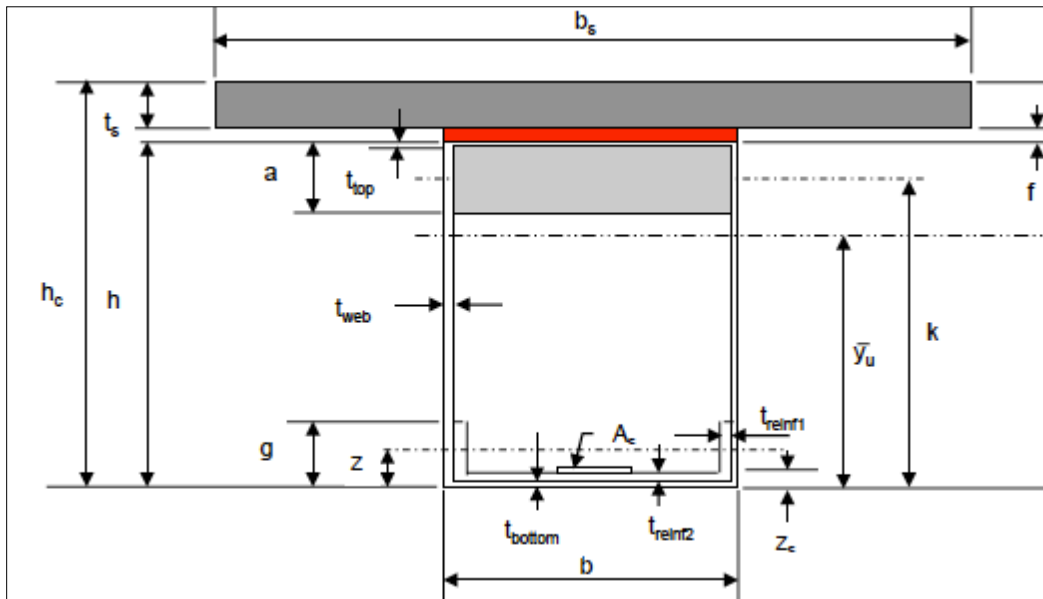
Figure 3. Ports for injecting SCC.



Figure 4. Interior view of a concrete-filled HCB.



Figure 5. Cross section geometry of a typical HCB.



Load rating factors were obtained by using the guidelines specified in the American Association of State Highway and Transportation Officials (AASHTO) Manual for Bridge Evaluation (MBE) (AASHTO 2011) and the Kentucky Transportation Cabinet's Transmittal Memo TM 08-01, issued to promulgate the revision of "Chapter 4, Interpretation of LRFD" (Load

and Resistance Factor Design; Frank 2008). Member capacities were calculated based on provided design drawings and calculations, the AASHTO specifications, and the results of the laboratory-scale testing performed on this type of HCB. Load testing measurements alone do not provide a complete picture of the bridge's performance. Measured responses are generally limited to the sensor locations, which may not be at the controlling location for member response. Use of a finite-element model allowed for the evaluation of all components of the structure for a variety of response types such as moment and shear. For example, strain measurements can provide a reasonably direct measure of applied moment at a given location, but it is very difficult to measure shear directly. Moment and shear at all locations along each beam-line can be evaluated through finite-element analysis (FEA) modeling. An initial quasi-three-dimensional model accurately matched measured displacements and strain shape near midspan, but the rotations and strain shapes near the supports did not agree with the measurements. This model assumed composite action between the concrete and GFRP shells. Calibration efforts failed to produce agreement with the measured data at the supports. A full three-dimensional (3D) model did not force continuity, and it was found to better simulate the interaction between the concrete arches and GFRP shells (Commander and Carpenter 2016 for modeling details). This 3D model, along with the field testing and design calculations, was used to determine the HCB load capacity.

2.2 Field work

The existing 82-foot long Bridge No. 4 was demolished to remove the existing road deck and support beams for the two spans. Demolition was done by the Fort Knox DPW and its support contractor, All Cities Enterprises of Fort Knox, Kentucky. The abutments and pier were not removed, but they were rehabilitated by forming and pouring new concrete landings for the new support beams. The condition of the support beam structures, as visible during demolition, is shown in Figure 6 and Figure 7.

Figure 6. Corroded support beam structure visible during demolition.



Figure 7. Lifting degraded steel beam structure during demolition.



After demolition of the deck and support beams, the bridge's support began to be restored with use of the demonstrated HCB technology. HCBs were procured that were specially designed for one of the spans of Bridge No. 4. The beams were fabricated offsite and shipped to Fort Knox. The new HCBs were delivered to the site (Figure 8) without the compression reinforcement arch in the beam. These beams were designed to be filled with SCC on site to make the compression reinforcement arch. The SCC was slump tested at the site (Figure 9) and then poured into the HCBs to cast the arch prior to installation of the beams (Figure 10). Lifting loops were on the HCBs for lifting at the ends of the beam following casting of the compression reinforcement arch (see loops showing at top of beam in Figure 8). Once cured, the beams were lifted and placed on the pier and abutment for the north-facing span of the bridge (Figure 11–Figure 13). A conventional rebar reinforced bridge deck was constructed over the HCBs,

with two rows of rebar installed in a 4-inch grid pattern and a 3-inch separation between rows (Figure 14 and Figure 15). The top row maintained a 1.75-inch clearance from the surface of the deck. Sensors were placed in the bridge deck to measure site corrosivity (see sections 3.1.1). The completed bridge span is shown in Figure 16. When completed, the bridge was load-tested to assess the structural integrity and then retested after 1 year (see 3.1.2). Details of these tests are in another report, ERDC/CERL CR-16-5 (Commander and Carpenter 2016).

Figure 8. HCB as delivered to site.



Figure 9. Slump test of SCC.



Figure 10. Casting the internal compression reinforcement arch.



Figure 11. Span of Bridge No. 4 (foreground) prior to installing HCBs.



Figure 12. Crane lifting an HCB for installation.



Figure 13. Placing an HCB.



Figure 14. Forming bridge deck and installing rebar.



Figure 15. Bridge deck construction in progress.



Figure 16. Completed bridge No. 4 with HCBs (left) and Gridform deck on Cor Ten® weathering steel beams (right).¹



2.3 Commissioning and monitoring

The evaluation of the HCBs was accomplished by conducting two load tests on Bridge No. 4. Construction of the bridge, including the HCBs, was completed in October 2012, but the guard rails and approaches to the bridge were not finished until December 2012. Only at that time could the initial load test be scheduled and conducted, and the final load test was conducted in December 2013. This evaluation assessed the performance of the HCBs and verified that the bridge meets design load requirements. The load tests were performed by subcontractor Bridge Diagnostics Inc. of Boulder, Colorado (Figure 17 and Figure 18). The instrumentation plan and other details of the monitoring and testing are located in the subcontractor's full report, ERDC/CERL CR-16-5 (Commander and Carpenter 2016).

¹ Cor-Ten is a registered trademark of U.S. Steel for a weathering steel product that forms a passivating surface layer of oxidized material that protects the steel element from progressive corrosion. More information is available in ERDC/CERL TR-16-21, which discusses material selection for the bridge span used to demonstrate the composite Gridform® concrete deck reinforcement system.

Figure 17. Weighing a truck to be used for load testing.



Figure 18. Two-lane load testing.



An evaluation of the corrosion potential of the site was done with the use of a weather station, the corrosion sensors embedded in the concrete deck, and an atmospheric corrosion test rack. The site was also visited quarterly, with weather station data downloaded and readings taken from the corrosion sensors. At six and twelve months, coupons were retrieved from the corrosion test rack and assessed by a laboratory. Establishment of the site corrosion potential is used to evaluate the potential future performance of the HCB materials. Appendix B provides a summary of the data recorded for the corrosion potential and an interpretation of the results to form the site corrosion potential.

3 Discussion

3.1 Results

3.1.1 Site corrosivity

A summary of the data and calculations to determine site corrosivity are listed in Table 1–Table 4.

The results from the ISO 9223:2012 analysis of weather data (Table 1) and mass loss testing suggest the Fort Knox Bridge No. 4 site is a C3 classification of atmospheric corrosion severity. Although the steel coupon testing resulted in a C2 classification, the results were on the upper limit of the category. The potential for corrosion at the site is considered medium. The corrosion sensors show no corrosion in the bridge and validate this classification as being much less than severe.

Copper experienced a high mass loss in comparison to the other metals in both the 6-month and 12-month tests (Table 2 and Table 3). Results from the 12-month testing suggest that the 2024 and 7075 aluminum alloys experienced an extremely high mass loss due to corrosion. These results are inconsistent with the other alloys and the results from the weather data analysis; therefore, the mass loss test from the 12-month 2024 and 7075 coupon have been omitted from the atmospheric corrosion severity classification of the site (Table 4).

Table 1. Summary of weather data collected December 2012 – December 2013.

	Wind Direction, ϕ	Wind Speed, mph	Gust Speed, mph	Temp, °F	RH, %
Average	192	0.25	2.5	56.3	83.2
Standard Deviation	100	0.91	3.6	18.1	18.9

Table 2. Summary of results from the 6-month ASTM G1 mass loss test and corrosion classification per ISO 9223:2012.

	1010 Steel	CDA101	Al6061-T6	Al2024-T3	Al7075-T6
Weight loss [g]	0.104	0.417	0.005	0.003	0.005
Rcorr [g/m ² y]	37.71	151.66	1.95	0.94	1.74
Classification	C2 (Low)	CX (Extreme)	C3 (Med)	C3 (Med)	C3 (Med)

Table 3. Summary of results from the 12-month ASTM G1 mass loss test and corrosion classification per ISO 9223:2012.

	1010 Steel	CDA101	Al6061-T6	Al2024-T3	Al7075-T6
Weight loss [g]	0.984	0.143	0.006	0.294	0.192
Rcorr [g/m ² y]	178.9	25.91	1.05	53.36	34.96
Classification	C2 (Low)	C5 (Very High)	C3 (Med)	CX (Extreme)	CX (Extreme)

Table 4. Atmospheric corrosion severity classification from weather data and ISO 9223:2012 response equation calculations.

	Steel	copper	aluminum	zinc
Rcorr [$\mu\text{m}/\text{y}$]	9.67	0.88	0.04	0.54
Classification	C2 (Low)	C3 (Med)	-	C2 (Low)

3.1.2 Load testing

The HCBs used at Fort Knox Bridge No. 4 were load tested in December 2012 and a year later in December 2013. These tests provided performance verification, which is needed for bridges built with innovative structural materials. Details on the load testing, FEA modeling, and rating of the HCB bridge span are contained in the contractor's report, published as ERDC/CERL CR-16-5 (Commander and Carpenter 2016). The following are brief highlights from the full report:

- A post processor was used to sift through the various analysis output files, and it generated load rating factors for every component. The ratings were calculated and assembled for the critical responses generated from the bridge model for the different load components used in the AASHTO LRFD rating equations. A summary of the calculated HCB capacities used in strength and serviceability ratings, along with important member properties, have been provided in Table 5–Table 9.
- Load and resistance factor ratings (LRFs) were calculated using the AASHTO load-rating equation specified in the MBE.
- Member shear and moment capacities were based on AASHTO LRFD specifications to the extent that they applied. Additional laboratory test data was used for the HCB beams to establish the controlling failure mechanism.
- Different models were used to compute the various load effects for component dead load (DC), superimposed dead load (DW), and live-load (LL).
- Dead-loads were computed from simply supported noncomposite versions of the bridge model.

- The calibrated FEA model was used to generate live-load responses for the HL-93 design load and the required military loads.
- Unreliable secondary stiffness parameters resulting from the load test and model calibration were removed from the model prior to load rating. For example, additional edge stiffening provided by the guard rails was removed. Observed friction at the beam bearings, which resulted in beam rotational end-restraint, was reduced because it could change over time and may not exist at higher load levels. The goal was to ensure load ratings would be conservative.
- Two-lane loading was used for design loads.
- The large military loads were considered permit loads due to loading frequency and the bridge's traffic count. Only single-lane loading was applied with the Military Load Classification (MLC) loads due to the bridge width.

In all cases, the rating results for the HCBs were controlled by shear in the GFRP webs under the single-lane loaded condition, with the rating load close to the exterior girder. The HCB sections met all of the Inventory and Operating level rating criteria (rating factor [RF] >1.0) for all load configurations. The controlling rating was found to be the HL-93 inventory-level shear rating of 1.76 for an exterior girder approximately 12 feet from the bearing location.

The HCB span's controlling MLC tracked rating was a MLC-139 based on an M1A1 Abrams tank load that had an RF of 1.94. The controlling MLC wheeled rating was determined to be MLC-212, which was based on the MLC-70 wheeled vehicle that had an RF of 3.04. Lastly, the service-level rating indicated that the HCB arches will not crack under the HETS service level loads. Although this rating was not a standard AASHTO rating consideration, it helps verified that there should not be a serviceability concern with respect to the concrete portion of the HCBs.

The steel girders met both inventory and operating rating criteria (RF >1.0) for all load configurations (Table 5) and also met the rating criteria for HL-93. The critical rating factor for HL-93 loading condition was controlled by positive flexure of the center girder at midspan. The HL-93 load rating was controlled by the two lanes loaded condition of the Design Tandem + Lane load configuration centered on the bridge. Under the fatigue loading condition and all military loads, the controlling member was the

first interior girder because the single lane edge loading most directly loaded this beam.

The steel girder span's controlling tracked vehicle load limit was MLC-184 based on an M1A1 Abrams operating rating of 2.55. However, the HCB span had a lower tracked MLC rating of 139 tons and therefore, that rating controlled Bridge No. 4's load capacity. The controlling responses for the HCB span are provided in the tables below (Table 5–Table 8). Additionally, tonnage ratings are provided in Table 9 for all rated military loads. A comparison between the final 2012 calibrated model and the data collected during the second round of tests indicated that the structural behavior did not significantly change over one year's time.

Table 5. Controlling rating factors and responses—girders in shear (MEC).

Loading Condition	Controlling Location	DC Moment. KIP-IN	DC Moment. KIP-IN	DC Moment. KIP-IN	Inventory RF	Operating RF
HL-93 (Strength)	Center steel girder/at midspan	1441.90	754.34	2854.06	2.42	3.14
HL-93 (Service)	Center steel girder/at midspan	1441.90	754.34	2854.06	2.85	3.70
HL-93 (Fatigue)	Interior steel girder/at midspan	0.0	0.00	1325.22	5.68	—
HETS M1070/M1000	Interior steel girder/at midspan	1392.20	778.57	2754.21	2.49	3.23
HETS M1070/M747	Interior steel girder/at midspan	1392.20	778.57	3236.24	2.14	2.77
M1A1 Tracked	Hybrid span deck force/ at midspan	1.36	0.61	4.64	—	2.64
MLC70 Wheeled	Interior steel girder/at midspan	1392.20	778.57	3382.00	—	3.52

Note: Dead-load responses are unfactored. Live-load responses have applicable multiple presence factors applied, but not the impact factor. HL-93 responses account for 25% load amplification on the truck load.

Table 6. Strength rating factors and responses—HCBs in positive flexure (Table 4.5 in Commander and Carpenter 2016).

Loading Condition	Controlling Location	DC Response .KIP-IN	DC Response .KIP-IN	DC Response .KIP-IN	Inventory RF	Operating RF
HL-93 (Strength)	Exterior girder/at midspan	-1.36	-0.61	-3.68	2.47	3.20

¹ A "kip" is one kilopound of force.

Loading Condition	Controlling Location	DC Response .KIP-IN	DC Response .KIP-IN	DC Response .KIP-IN	Inventory RF	Operating RF
HETS M1070/M1000	Exterior girder/at midspan	-1.36	-0.61	-3.28	2.77	3.60
HETS M1070/M747	Exterior girder/at midspan	-1.36	-0.61	-3.68	2.47	3.20
M1A1 Tracked	Exterior girder/at midspan	-1.36	-0.61	-4.47	—	2.63
MLC70 Wheeled	Exterior girder/at midspan	-1.36	-0.61	-2.97	—	3.98

Note: Dead-load responses are unfactored. Live-load responses have applicable multiple presence factors applied, but not the impact factor. HL-93 responses account for 25% load amplification on the truck load.

Table 7. Controlling tonnage rating factors for all military loads (Table 4.8 in Commander and Carpenter 2016).

Loading Condition	Controlling Location	DC Shear, KIP	DC Shear, KIP	DC Shear, KIP	Inventory RF	Operating RF
HL-93 (Strength)	Center steel girder/near end	13.06	5.73	32.74	6.39	8.29
HETS M1070/M1000	Interior steel girder/ near end	13.01	5.77	33.00	6.34	8.20
HETS M1070/M747	Interior steel girder/ near end	13.01	5.77	37.25	5.62	7.28
M1A1 Tracked	Hybrid girder/ GRFP web	0.24	0.20	1.20	—	1.94
MLC70 Wheeled	Hybrid girder/ GRFP web	0.19	0.22	0.98	—	3.04

Note: Dead-load responses are unfactored. Live-load responses have applicable multiple presence factors applied, but not the impact factor. HL-93 responses account for 25% load amplification on the truck load.

Table 8. Controlling strength rating factors and responses—HCBs in shear limited by GFRP shells (Table 4.7 in Commander and Carpenter 2016).

Loading Condition	Controlling Rating Factor	Controlling Location	DC Shear; KIPS	DW Shear; KIPS	LL Shear; KIPS
HL-93 (Inventory)	1.76	Exterior beam/ ~12' from bearing	4.25	2.03	13.35
HL-93 (Operating)	2.28				
HETS M1070/M1000 (Inventory)	2.22	Exterior beam/ ~10' from bearing	5.28	2.05	10.22

Loading Condition	Controlling Rating Factor	Controlling Location	DC Shear, KIPS	DW Shear, KIPS	LL Shear, KIPS
HETS M1070/ M1000 (Operating)	2.88				
HETS M1070/ M747 (Inventory)	1.80	Exterior beam/ ~12' from bearing	4.26	2.02	13.02
HETS M1070/ M747 (Operating)	2.34				
M1A1 Tracked	1.94	Exterior beam/ ~11' from bearing	4.78	2.06	15.43
MLC70 Wheeled	3.04	Exterior beam/ ~11' from bearing	4.78	2.06	9.83

Note: Provided shear values have been converted from kips/m (related to the GFRP shell elements) into units of kips for clarity. Dead load responses are unfactored. Live-load responses have applicable multiple presence factors applied but not the impact factor. HL-93 responses account for 25% load amplification on the truck load.

Table 9. Controlling tonnage rating factors for all military loads (Table 4.8 in Commander and Carpenter 2016).

Loading Condition	Controlling Location/ Capacity	Inventory RF (tons)	Operating RF (tons)
HETS M1070/ M1000	Exterior beam ~10' from bearing/shear	255	331
HETS M1070/ M747	Exterior beam ~12' from bearing/shear	189	245
M1A1 Tracked	Exterior beam ~11' from bearing/shear	—	139
MLC70 Wheeled	Exterior beam ~11' from bearing/shear	—	212

3.2 Lessons learned

Even though HCBs are a novel and emerging technology, this demonstration project was accomplished without any need for special tooling or methods. Prior to installing the beams, it was an easy process to pour the SCC onsite into the HCBs to form the reinforcing arch. Because of the light weight of the demonstrated technology compared with conventional beams, the HCBs are easier to ship and place than conventional precast bridge beams.

The only additional material or hardware required for installation of the beams were steel lifting loops, which have to be installed at the ends of

HCBs that have not been lifted into place when the SCC is being poured. However, if the beams are in their final position when the SCC is poured, the lifting loops are not required.

4 Economic Summary

4.1 Costs and assumptions

ERDC-CERL was unable to obtain detailed information from the contractor about any productivity increase during beam installation. Based on observations from the field, construction of the bridge using the HBC went according to plan, with no additional work or tasks identified. As a result, the original assumptions developed for this project are assumed to be correct. The original cost estimates have been revised to reflect actual project costs (Table 10 and Table 11).

Table 10. Breakdown of total project costs.

Description	Amount, \$K
Labor	78.2
Support from Fort Knox for bridge construction	440.0
Cost for Beams	150.0
Cost for Chloride Sensors	15.1
Contract for monitoring and testing	146.7
Travel	25.0
Reporting	20.0
Air Force and Navy participation	5.0
Total	880.0

Table 11. Project field monitoring costs.

Item	Description	Amount, \$K
1	Labor for project management and execution	70.8
2	Travel for project management	17.0
3	Cost for materials	7.6
4	Cost for corrosion analysis	10.9
5	Cost for load tests	40.4
	Total	146.7

Alternative 1 (Standard Reinforced Concrete Bridge). The scenario assumes that in year 2, four reinforced concrete bridges are replaced at \$4 million each. These four conventional bridges will need \$1 million in major repairs 8 years later and \$2 million in major repairs again 8 years after that. Due to corrosion degradation, the four conventional bridges will need to be replaced completely in year 26.

Alternative 2 (Bridge Rehabilitation With HCBs). As above, this scenario assumes that four reinforced-concrete bridges are replaced in year 2 (at \$4 million each), using the HCBs instead of conventional steel or reinforced concrete beams. The higher cost of the HCBs are assumed to be offset by cost savings in transportation and constructability due to their lighter weight. Project investment covers the cost of the HCBs for one bridge, reducing the total year-one costs by \$150,000. Then, 20 years later, the HCBs are assumed to need some minor repair at a cost of \$50,000 per bridge. This repair, however, extends bridge service life for another 20 years (total life span of 45 years). At year 26, only the bridge decks will need replacement at a cost of \$325,000 each.

4.2 Projected return on investment (ROI)

Over 30 years, using the methods prescribed by OMB Circular A-94 (OMB 1992) and the above assumptions, the projected ROI for this demonstration is 4.22 (Table 12). This return is lower than the 19.9 ratio computed in the original project management plan (PMP), which used unrealistic assumptions for Alternative 2, such as replacing just the beams on a deteriorated bridge. The original calculation also left off replacement of the bridge decks at year 26. While deck replacement is not linked to the durability of HCBs, it is nonetheless an expense of Alternative 2 over the 30-year life cycle.

Table 12. Return on investment calculation.

Return on Investment Ratio	4.22	Percent	422%
Net Present Value of Costs and Benefits/Savings	14,112	17,830	3,717

A Future Year	B Baseline Costs	C Baseline Benefits/Savings	D New System Costs	E New System Benefits/Savings	F Present Value of Costs	G Present Value of Savings	H Total Present Value
1							
2	16,000		15,850		13,843	13,974	131
3							
4							
5							
6							
7							
8							
9							
10	1,000					508	508
11							
12							
13							
14							
15							
16							
17							
18	2,000					592	592
19							
20							
21							
22			200		45		-45
23							
24							
25							
26	16,000		1,300		224	2,755	2,531
27							
28							
29							
30							

5 Conclusions and Recommendations

5.1 Conclusions

HCBs are a novel and emerging technology that show great promise for corrosion reduction when used in standard concrete-deck bridge spans such as the one that was the subject of this demonstration. Even though the beam design differs dramatically from conventional bridge beams, the HCBs were installed using standard construction equipment and tools. Procedures for installation of the beams differ, as reported in Chapter 2, but the methods fall within the skill set of conventional construction crews and managers. The lighter weight of the demonstrated technology, as compared with conventional beams, offer advantages in terms of lower shipping weight and reduced equipment requirements for hoisting beams into place.

The summary of load testing results (summarized in section 3.1.2) shows that the HCB span met all operating level ratings. The service level ratings indicated that the HCB arches will not crack under the HETS service level loads. While this rating was not a standard AASHTO rating consideration, it helped to verify that there should not be a serviceability concern with respect to the concrete portion of the HCBs.

In general, the response data recorded during the load tests was found to be of good quality. Responses collected during the first occurrence of a heavier load indicated some girder movement at the bearing and bridge rail locations. This behavior was most likely a function of friction between the elastomeric bearing pads on the bottom of the beams. A small amount of movement can be expected with heavy vehicles and significant temperature changes. The responses were observed during the first crossing of each heavy vehicle and then disappeared with repeated tests.

The bridge and the resulting 3D model exhibited excellent lateral load transfer characteristics and a small level of continuity between spans. In general, the noncomposite slab and girders behaved as expected. A small amount of friction-induced end restraint was observed during both rounds of tests. Additionally, the exterior girders behaved partially compositely with the edge of the slab and guard rail due to the connection detail. It was assumed the end-restraint and partially composite behavior may not exist

indefinitely, particularly with heavy loads approaching the bridges ultimate capacity. Therefore the calibrated model was altered by removing these secondary stiffness parameters to provide a more conservative load-rating model.

Load ratings were computed using an altered version of the calibrated model that was considered to be more reliable for rating. In all cases the rating results for the HCBs were controlled by shear in the GFRP webs. The beams met rating criteria ($RF > 1.0$) for all specified loads and rating levels. Additionally, the HCB span was limited by a 139-ton tracked vehicle and 212-ton wheeled vehicle, which controlled Bridge No. 4's MLC ratings.

5.2 Recommendations

5.2.1 Applicability

HCBs should be considered as alternatives to conventional steel or reinforced concrete beams for all girder-type bridges used on Army and DoD Installations. Due to the polymer composite protective shell, this is especially true for locations of high corrosivity such as coastal regions or where road salts are used in the winter months.

5.2.2 Implementation

According to Unified Facilities Criteria (UFC) 3-301-01, *Structural Engineering*, highway bridges shall be designed in accordance with AASHTO HS-20 and "LRFD (Load and Resistance Factor Design) Bridge Design Specifications." AASHTO Subcommittee T-6, Fiber Reinforced Polymer Composites, is aware of this technology but, at present, considers hybrid composite bridge beams to be a niche product. However, as validated in this demonstration, AASHTO specifications can be applied in conjunction with manufacturer instructions to successfully use this technology.

There is currently no guidance in any UFC or Unified Facilities Guide Specification (UFGS) documents with regard to use of FRP composites. Under an FY15-funded project, "Composites for Bridge Application," ERDC-CERL is developing a new UFC for the use of FRP composites in bridge structures. FRP composite reinforcing elements, such as the HCBs, will be included in this new guidance. Publication of this new UFC is expected in 2017. This guidance should facilitate wider use of FRP composites for bridge applications in advance of future AASHTO guidance.

References

- AASHTO. 2011. *Manual for Bridge Evaluation, 2nd Edition*. Washington, DC: American Association of State Highway and Transportation Officials.
- ASTM B825-02. 2008. "Standard Test Method for Coulometric Reduction of Surface Films on Metallic Tests." West Conshohocken, PA: ASTM International.
- ASTM G1-03. 2011. "Standard Practice for Preparing, Cleaning and Evaluating Corrosion Test Specimens." West Conshohocken, PA: ASTM International.
- Commander, Brett, and Brice Carpenter. 2016. *Field Testing and Load Rating Report for Bridge No. 4, Hybrid Composite Beam Span, at Fort Knox, Kentucky: Contractor's Supplemental Report for Project F12-AR15*. ERDC/CERL CR-16-5. Champaign, IL: ERDC-CERL.
- Dean, Mike. 2008. "Bridges on Army Installations." In *Structural Health Management of Steel and Composite Bridges* (p 4), workshop presentation hosted by ERDC-CERL for Department of Defense, Corrosion Prevention and Control program, 1–2 May 2008 in Crystal City, Virginia.
- Frank, Allan W. 18 July 2008. "Transmittal Memorandum 08-01," subject: Chapter 4 in *Division of Structural Design Guidance Manual*, (rev. of Chapter 4, "Interpretation of AASHTO LRFD Specifications"). Frankfort, KY: Kentucky Transportation Cabinet, Director of Division of Structural Design. <http://transportation.ky.gov/Structural-Design/Pages/Transmittals-Memorandas.aspx>.
- Hastak, M., D. Halpin, and T. Hong. November 2004. *Constructability, Maintainability, and Operability of Fiber Reinforced Polymer (FRP) Bridge Deck Panels*. Joint Transportation Research Program, Project No. C-36-56NNN (FHWA/IN/JTRP-2004/15). West Lafayette, IN: Purdue University.
- HC Bridge Company, LLC. n.d. "Hybrid Composite Beam (HCB) Technology." Part of a two-page ACEC National Engineering Excellence Grand Award Winner brochure for Long Run Creek bridge, constructed in 2008 by Teng & Associates of Chicago, IL. Alpharetta, GA: HC Bridge Company, LLC.
- Hillman, John R. PE, SE. 2012. *Hybrid-Composite Beam (HCB®) Design and Maintenance Manual*. Prepared for Missouri Department of Transportation. Alpharetta, GA: Hillman, Inc.
- ISO 9223. 2012. "Corrosion of Metal and Alloys – Corrosivity of Atmospheres – Classification, Determination and Estimation." Geneva, Switzerland: International Standards Organization.
- Koch, G.H., P.H. Brongers, N.G. Thompson, Y.P. Virmani, and J.H. Payer. March 2002. *Corrosion Costs and Prevention Strategies in the United States*. Report No. FHWA-RD-01-156. Washington, DC: Federal Highway Administration.

OMB (Office of Management and Budget). 1992. "Guidelines and Discount Rates for Benefit-Cost Analysis of Federal Programs." OMB Circular No. A-94. Washington, DC: Office of Management and Budget.

Sweeney, Steven C., Richard G. Lampo, James Wilcoski, Christopher Olaes, and Larry Clark. 2016. *Demonstration and Validation of a Composite Grid Reinforcement System for Bridge Decks: Final Report on Project F12-AR01*. ERDC/CERL TR-16-21. Champaign, IL: ERDC-CERL.

UFC 3-301-01. 2010. *Structural Engineering*. Washington, DC: Department of Defense, www.wbdg.org.

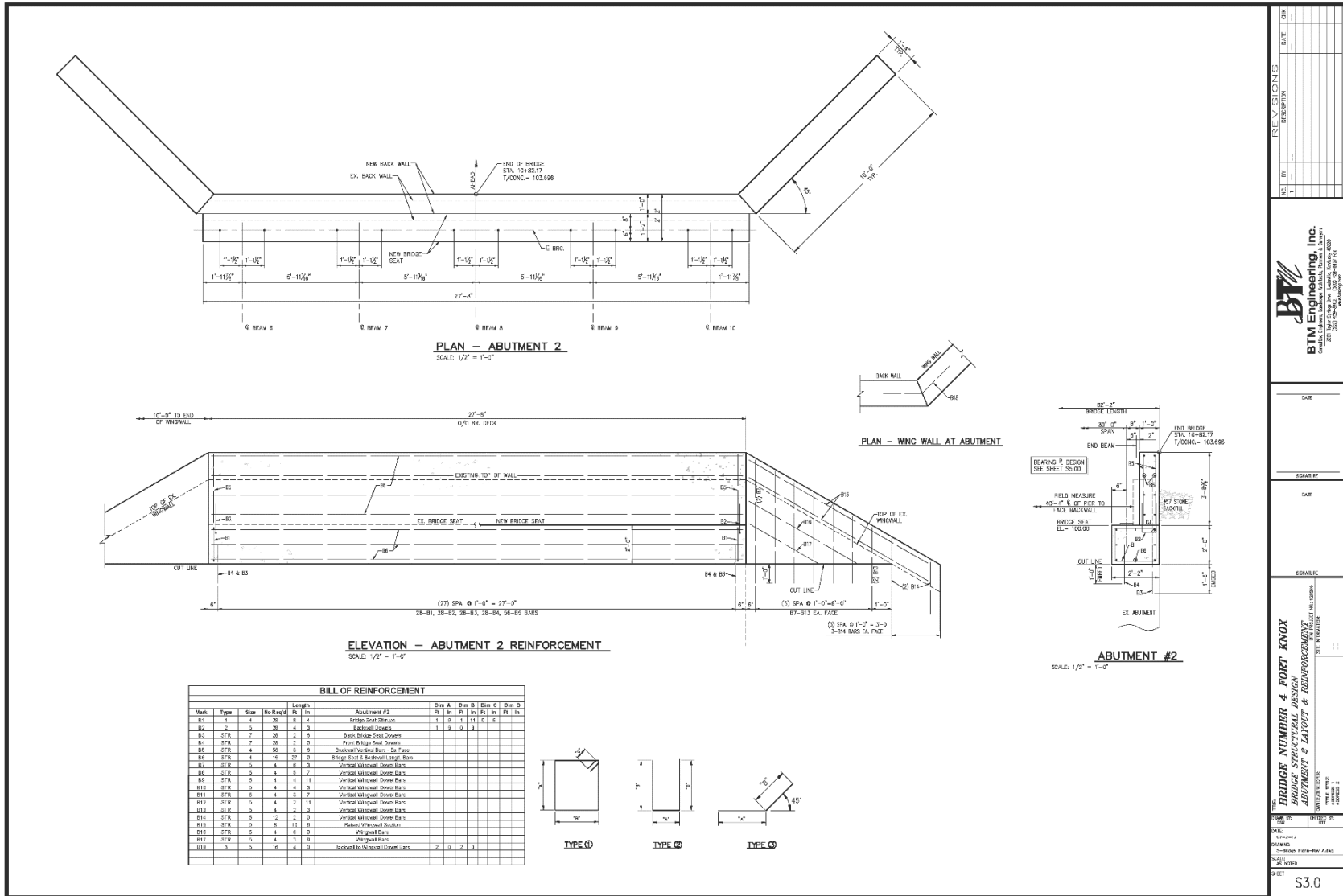
(This page intentionally blank.)

Appendix A: Engineering Drawings for Bridge No. 4, Fort Knox, Kentucky

Appendix A contains the engineer design and specification drawings as prepared by Bridge Diagnostics, Inc. for both of the demonstrated and evaluated spans of Bridge No. 4 at Fort Knox, Kentucky.

Bridge Diagnostics, Inc. did not produce separate drawings for each span; therefore, all the drawings are included in Appendix A, covering both the hybrid composite bridge beams span (this report) and the composite grid reinforcement system span, which is the subject of ERDC/CERL TR-16-21 (Sweeney et al. 2016).

Figure A4. Engineer drawing for Abutment 2 on Bridge No. 4, Fort Knox.



REVISIONS	
NO.	DESCRIPTION

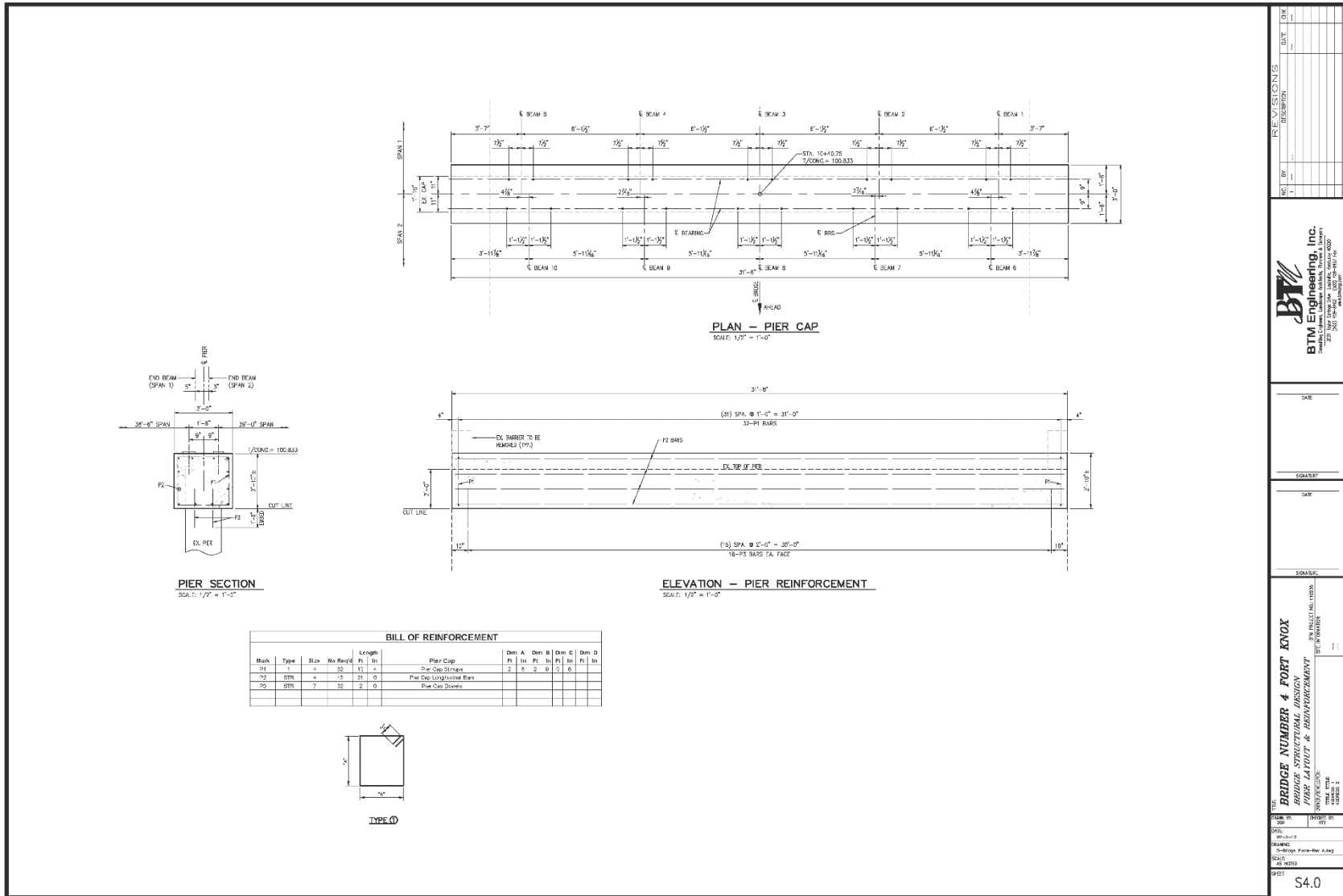
BTM Engineering, Inc.
 1000 W. 10th Street, Suite 100
 Fort Collins, CO 80521
 (970) 221-1111
 www.btmeng.com

DATE: _____
 DRAWN BY: _____
 CHECKED BY: _____
 DESIGNER: _____
 APPROVED BY: _____

BRIDGE NUMBER 4 FORT KNOX
BRIDGE STRUCTURAL DESIGN
ABUTMENT 2 LAYOUT & REINFORCEMENT

DATE: 07-23-12
 DRAWN BY: Fort-Hill-A-Eng
 SCALE: AS SHOWN
 SHEET: S3.0

Figure A5. Engineer drawing for bridge pier on Bridge No. 4, Fort Knox.



REVISIONS	
NO.	BY
1	
 BTM Engineering, Inc. 1000 N. 10th St., Suite 100 Fort Worth, TX 76102 (817) 342-1000 www.btmeng.com	
DATE	
SCALE	
DATE	
COMPILE	
BRIDGE NUMBER 4 FORT KNOX BRIDGE STRUCTURAL DESIGN PIER LAYOUT & REINFORCEMENT DATE: 08-23-17 DRAWN: Fort-Knox-A.dwg SCALE: 1/2" = 1'-0" SHEET: S4.0	

Appendix B: Corrosion Potential Assessment for Bridge No. 4, Fort Knox, Kentucky

Classification method

A corrosion severity classification for the Bridge #4 site at Fort Knox was developed for use in evaluating the materials used in this project. This was accomplished at the site through placement of a portable weather station (collecting weather data for one year), an atmospheric corrosion test rack, (equipped with sensors to monitor corrosion and chlorides were inserted in the bridge deck), and quarterly site visits (performed visual inspections).

Monitoring

Weather station

A weather station was installed to measure and record environmental characteristics throughout the exposure period as shown in Figure B1. The station measured temperature, relative humidity, wind speed and direction, and rainfall. The weather station was powered by a solar panel and a rechargeable battery. A data logger was used to store the measurements which were recorded every 12 hours by the rain gage and every 15 minutes for the remaining sensors. Data was downloaded manually during each quarterly inspection through the use of a laptop computer. The data logger has a storage capacity to continue storing data at 15-minute intervals for approximately 2.5 years. Upon reaching full capacity, the data logger will truncate the oldest data point to create room for new, incoming data.

Figure B1. Weather station.



Sensors

Sensors were installed in the bridge deck to measure chloride penetration, corrosion potential, and corrosion rate (Figure B2). Measurements from the sensors were taken quarterly for a 12-month period.

The Rohback Cosasco 900 Concrete Multi-Depth Sensor was utilized to accomplish the chloride measurements. Four sets of electrodes are spaced by 1 in. intervals to provide four separate measurements at different depths from each sensor. The 900 sensors were mounted such that the first electrode was 1 in. from the surface of the concrete. Two sensors were positioned in the span with the RFP reinforcement, and three sensors were positioned in the control span adjacent to it. The Rohback Cosasco Aquamate was used to collect the corrosion rate measurements.

The Borin Stelth 7 sensor was used to measure corrosion potential in the bridge deck. The Stelth 7 sensor is an IR-Free probe with a silver-silver chloride (Ag-AgCl) electrode. Corrosion potential sensors measure a voltage difference between the sensor electrode and reinforcement rebar; therefore six Stelth 7 sensors were installed only throughout the control span of the bridge. Two ground wires were installed for redundancy. Measurements from each ground should theoretically be identical. An Extech 540 multimeter was used to collect the corrosion potential measurements.

Rohback Cosasco 800 LPR Corrosion Rate sensors were used to measure the instantaneous corrosion rate of reinforcing steel in concrete by the method of Linear Polarization Resistance (LPR). The electrodes of the LPR probe are manufactured using carbon steel. The LPR sensor utilizes the solution resistance compensation (SRC) method which makes a separate measurement and correction for the effect of the resistivity of the concrete and eliminates the need for a third electrode that is typically used in LPR sensors. Five LPR sensors were positioned throughout the control span of the bridge. The Rohback Cosasco Aquamate was used to collect the imbalance (Imb) measurements.

Sensor types and locations are in BDI's full report, contained in ERDC/CERL CR-16-5 (Commander and Carpenter 2016).

Coupons to simulate chloride penetration

A concrete coupon was formed in a 5-gallon bucket to provide a method to simulate chloride penetration. The bucket was filled approximately half-way with a concrete mix including one cup of sodium chloride. A corrosion ladder was situated in the form such that the chloride enriched concrete covered the first two set of electrodes of the chloride sensor. A corrater was also submerged in the concrete. The concrete was provided 24 hours to cure before filling the rest of the form with standard concrete. Figure B2 shows the chloride-enriched concrete covering the corrater and half of the chloride ladder sensor. Figure B3 shows the cured concrete coupon. Measurements were collected during the quarterly inspections.

Figure B2. Coupon preparation.



Figure B3. Finished coupon.



An atmospheric coupon rack to determine the relative corrosivity of the site was installed facing 90 degrees from vertical at the bridge site (Figure B4). The corrosion coupons included silver, copper, 1010 steel, and three aluminum alloys (2024 T3, 6061 T6, and 7075 T6). The coupons measured 1 in. wide by 4 in. long by 1/16 in. thick. These coupons were collected after 6 months and 12 months of exposure. The mass of each coupon was recorded before being exposed to the test environment. The silver coupon was tested for chlorides in accordance with ASTM B825. The remaining coupons were analyzed for mass loss in accordance with ASTM G1-3.

Figure B4. Atmospheric corrosion test rack.



Assessments for weather, sensors, and corrosion coupon rack

Weather assessment

The weather data was analyzed using response functions from the ISO 9223:2012, “Corrosion of Metal and Alloys – Corrosivity of Atmospheres – Classification, Determination and Estimation.” SO_2 measurements were not collected; however due to the location of Bridge #4, it was assumed that deposition of SO_2 would be equal to zero milligrams per square meter, per day. The amount of Cl deposition was calculated from the ASTM B825, Standard Test Method for Coulometric Reduction of Surface Films on Metallic Tests” on the silver mass-loss coupon. The equations used are shown in Figure B6. Corrosion classifications per ISO 9223:2012 are shown in Table B1.

Figure B6. ISO 9223:2012 response equations for four standard metals.

Equation (1) for carbon steel:

$$r_{\text{corr}} = 1,77 \cdot P_d^{0,52} \cdot \exp(0,020 \cdot \text{RH} + f_{\text{St}}) + 0,102 \cdot S_d^{0,62} \cdot \exp(0,033 \cdot \text{RH} + 0,040 \cdot T) \quad (1)$$

$$f_{\text{St}} = 0,150 \cdot (T - 10) \text{ when } T \leq 10 \text{ }^\circ\text{C}; \text{ otherwise } -0,054 \cdot (T - 10)$$

$$N = 128, R^2 = 0,85$$

Equation (2) for zinc:

$$r_{\text{corr}} = 0,0129 \cdot P_d^{0,44} \cdot \exp(0,046 \cdot \text{RH} + f_{\text{Zn}}) + 0,0175 \cdot S_d^{0,57} \cdot \exp(0,008 \cdot \text{RH} + 0,085 \cdot T) \quad (2)$$

$$f_{\text{Zn}} = 0,038 \cdot (T - 10) \text{ when } T \leq 10 \text{ }^\circ\text{C}; \text{ otherwise, } -0,071 \cdot (T - 10)$$

$$N = 114, R^2 = 0,78$$

Equation (3) for copper:

$$r_{\text{corr}} = 0,0053 \cdot P_d^{0,26} \cdot \exp(0,059 \cdot \text{RH} + f_{\text{Cu}}) + 0,01025 \cdot S_d^{0,27} \cdot \exp(0,036 \cdot \text{RH} + 0,049 \cdot T) \quad (3)$$

$$f_{\text{Cu}} = 0,126 \cdot (T - 10) \text{ when } T \leq 10 \text{ }^\circ\text{C}; \text{ otherwise, } -0,080 \cdot (T - 10)$$

$$N = 121, R^2 = 0,88$$

Equation (4) for aluminium:

$$r_{\text{corr}} = 0,0042 \cdot P_d^{0,73} \cdot \exp(0,025 \cdot \text{RH} + f_{\text{Al}}) + 0,0018 \cdot S_d^{0,60} \cdot \exp(0,020 \cdot \text{RH} + 0,094 \cdot T) \quad (4)$$

$$f_{\text{Al}} = 0,009 \cdot (T - 10) \text{ when } T \leq 10 \text{ }^\circ\text{C}; \text{ otherwise } -0,043 \cdot (T - 10)$$

$$N = 113, R^2 = 0,65$$

where

r_{corr} is first-year corrosion rate of metal, expressed in micrometres per year ($\mu\text{m/a}$);

T is the annual average temperature, expressed in degrees Celsius ($^\circ\text{C}$);

RH is the annual average relative humidity, expressed as a percentage (%);

P_d is the annual average SO_2 deposition, expressed in milligrams per square metre per day [$\text{mg}/(\text{m}^2 \cdot \text{d})$];

S_d is the annual average Cl^- deposition, expressed in milligrams per square metre per day [$\text{mg}/(\text{m}^2 \cdot \text{d})$].

Table B1. Corrosion rates, r_{corr} , for the first year of exposure for the different corrosivity categories.

Corrosivity category	Corrosion rates of metals				
	Unit	Carbon steel	Zinc	Copper	Aluminium
C1	$\text{g}/(\text{m}^2\text{-a})$	$r_{\text{corr}} \leq 10$	$r_{\text{corr}} \leq 0,7$	$r_{\text{corr}} \leq 0,9$	negligible
	$\mu\text{m}/\text{a}$	$r_{\text{corr}} \leq 1,3$	$r_{\text{corr}} \leq 0,1$	$r_{\text{corr}} \leq 0,1$	—
C2	$\text{g}/(\text{m}^2\text{-a})$	$10 < r_{\text{corr}} \leq 200$	$0,7 < r_{\text{corr}} \leq 5$	$0,9 < r_{\text{corr}} \leq 5$	$r_{\text{corr}} \leq 0,6$
	$\mu\text{m}/\text{a}$	$1,3 < r_{\text{corr}} \leq 25$	$0,1 < r_{\text{corr}} \leq 0,7$	$0,1 < r_{\text{corr}} \leq 0,6$	—
C3	$\text{g}/(\text{m}^2\text{-a})$	$200 < r_{\text{corr}} \leq 400$	$5 < r_{\text{corr}} \leq 15$	$5 < r_{\text{corr}} \leq 12$	$0,6 < r_{\text{corr}} \leq 2$
	$\mu\text{m}/\text{a}$	$25 < r_{\text{corr}} \leq 50$	$0,7 < r_{\text{corr}} \leq 2,1$	$0,6 < r_{\text{corr}} \leq 1,3$	—
C4	$\text{g}/(\text{m}^2\text{-a})$	$400 < r_{\text{corr}} \leq 650$	$15 < r_{\text{corr}} \leq 30$	$12 < r_{\text{corr}} \leq 25$	$2 < r_{\text{corr}} \leq 5$
	$\mu\text{m}/\text{a}$	$50 < r_{\text{corr}} \leq 80$	$2,1 < r_{\text{corr}} \leq 4,2$	$1,3 < r_{\text{corr}} \leq 2,8$	—
C5	$\text{g}/(\text{m}^2\text{-a})$	$650 < r_{\text{corr}} \leq 1\ 500$	$30 < r_{\text{corr}} \leq 60$	$25 < r_{\text{corr}} \leq 50$	$5 < r_{\text{corr}} \leq 10$
	$\mu\text{m}/\text{a}$	$80 < r_{\text{corr}} \leq 200$	$4,2 < r_{\text{corr}} \leq 8,4$	$2,8 < r_{\text{corr}} \leq 5,6$	—
CX	$\text{g}/(\text{m}^2\text{-a})$	$1\ 500 < r_{\text{corr}} \leq 5\ 500$	$60 < r_{\text{corr}} \leq 180$	$50 < r_{\text{corr}} \leq 90$	$r_{\text{corr}} > 10$
	$\mu\text{m}/\text{a}$	$200 < r_{\text{corr}} \leq 700$	$8,4 < r_{\text{corr}} \leq 25$	$5,6 < r_{\text{corr}} \leq 10$	—

NOTE 1 The classification criterion is based on the methods of determination of corrosion rates of standard specimens for the evaluation of corrosivity (see ISO 9226).

NOTE 2 The corrosion rates, expressed in grams per square metre per year [$\text{g}/(\text{m}^2\text{-a})$], are recalculated in micrometres per year ($\mu\text{m}/\text{a}$) and rounded.

NOTE 3 The standard metallic materials are characterized in ISO 9226.

NOTE 4 Aluminium experiences uniform and localized corrosion. The corrosion rates shown in this table are calculated as uniform corrosion. Maximum pit depth or number of pits can be a better indicator of potential damage. It depends on the final application. Uniform corrosion and localized corrosion cannot be evaluated after the first year of exposure due to passivation effects and decreasing corrosion rates.

NOTE 5 Corrosion rates exceeding the upper limits in category C5 are considered extreme. Corrosivity category CX refers to specific marine and marine/industrial environments (see Annex C).

Table B2. Description of typical atmospheric environments related to the estimation of corrosivity categories.

Corrosivity category ^a	Corrosivity	Typical environments — Examples ^b	
		Indoor	Outdoor
C1	Very low	Heated spaces with low relative humidity and insignificant pollution, e.g. offices, schools, museums	Dry or cold zone, atmospheric environment with very low pollution and time of wetness, e.g. certain deserts, Central Arctic/Antarctica
C2	Low	Unheated spaces with varying temperature and relative humidity. Low frequency of condensation and low pollution, e.g. storage, sport halls	Temperate zone, atmospheric environment with low pollution ($\text{SO}_2 < 5 \mu\text{g}/\text{m}^3$), e.g. rural areas, small towns Dry or cold zone, atmospheric environment with short time of wetness, e.g. deserts, subarctic areas
C3	Medium	Spaces with moderate frequency of condensation and moderate pollution from production process, e.g. food-processing plants, laundries, breweries, dairies	Temperate zone, atmospheric environment with medium pollution (SO_2 : $5 \mu\text{g}/\text{m}^3$ to $30 \mu\text{g}/\text{m}^3$) or some effect of chlorides, e.g. urban areas, coastal areas with low deposition of chlorides Subtropical and tropical zone, atmosphere with low pollution
C4	High	Spaces with high frequency of condensation and high pollution from production process, e.g. industrial processing plants, swimming pools	Temperate zone, atmospheric environment with high pollution (SO_2 : $30 \mu\text{g}/\text{m}^3$ to $90 \mu\text{g}/\text{m}^3$) or substantial effect of chlorides, e.g. polluted urban areas, industrial areas, coastal areas without spray of salt water or, exposure to strong effect of de-icing salts Subtropical and tropical zone, atmosphere with medium pollution
C5	Very high	Spaces with very high frequency of condensation and/or with high pollution from production process, e.g. mines, caverns for industrial purposes, unventilated sheds in subtropical and tropical zones	Temperate and subtropical zone, atmospheric environment with very high pollution (SO_2 : $90 \mu\text{g}/\text{m}^3$ to $250 \mu\text{g}/\text{m}^3$) and/or significant effect of chlorides, e.g. industrial areas, coastal areas, sheltered positions on coastline

Section 3.1.1 of this report contains a summary of selected weather data collected from December 2012–December 2013 (Table 1), and the results from the response equation calculations (Table 4).

Sensor corrosion assessment

Data from sensors installed on the bridge were collected after 1, 4, 7, 10, and 13 months (Tables B3–B7). The zero, Corr, and Imb values at the bottom of each table represent instrument calibration check readings for a dummy probe provided by the CORRATER instrument manufacturer. The check values (5 ± 1 mpy [mils per year; 1 mpy = 0.001 in. per year] for corrosion rate and 0 ± 1 for imbalance) indicated that the instrument was functioning properly.

The CORRATER LPR probes at locations 1, 2, 3, and 5 all indicated very general and low general corrosion rates, ranging from 0–0.03 mpy. The imbalance readings (qualitatively indicative of pitting tendency) ranged from 0–0.02. Both of these sets of data indicate very low corrosion activity over the 13-month test period. This is not surprising because the corrosion

rate of steel in highly alkaline, uncontaminated concrete (pH ~ 13) is negligible due to the formation of a complex passive film (mixture of α and γ iron-oxide and magnetite). With sufficient concrete cover over the steel rebar and less severe corrosive environments, it can take more than a decade for corrosion rates to increase appreciably. The CORRATER probe at location number 4 indicated erratic corrosion rates; for example, ranging from "off scale" at 1 month, increasing to 13.8 mpy at 4 months, accelerating to 48.9 mpy at 7 months, then decreasing dramatically to 0.49 mpy at 10 months, and finally off scale again at 13 months. The imbalance readings were 0.39, 0.65, 0.48, 0.36, and 0.91, respectively. The imbalance readings were all lower than the corresponding general corrosion rates; thus, qualitatively indicating low pitting tendency. The check readings all indicated that the Aquamate CORRATER instrument was functioning properly. The results for the artificially-contaminated concrete block "salt coupon" are shown graphically in Figure 4. It is apparent that some corrosion activity was indicated at 4 months with an increase in pitting tendency at 7 and 10 months and a decrease at 13 months. Although the general corrosion rate appears to be increasing steadily, the actual rates (e.g., 0.04 mpy) are negligible.

For the chloride-ladders, the corrosion rates varied from 0–0.04 mpy and the imbalance readings from 0 to 0.07. The chloride-ladder at location 4 appeared to show the most activity. Although the imbalance readings were greater than the corrosion rates, all of the values were very small, indicating low corrosion activity. Similarly, the galvanic current measurements related to chloride ingress also indicated no significant penetration. The artificially-contaminated concrete block salt coupon exhibited the most activity at 1 and 4 months but this decreased dramatically at 7, 10, and 13 months possibly due to a drying out effect.

Table B3. Sensor data after 1 month.

Month 1 Data												
Location	1		2		3		4		5		Salt Coupon	
	Corr	Imbal	Corr	Imbal	Corr	Imbal	Corr	Imbal	Corr	Imbal	Corr	Imbal
Corrator	0.02	0	0	0	0.01	0.01	ovr	0.39	0.02	0.02	0.01	0
Location	1		4		5		FR1		FR2		Salt Coupon	
Chloride Ladders												
Corrosion	Corr	Imbal	Corr	Imbal	Corr	Imbal	Corr	Imbal	Corr	Imbal	Corr	Imbal
H	0	0	0	0.01	0	0	0	0	0	0	0	0
I	0	0	0	0.01	0	0	0	0	0	0	1.17	2.95
L	0	0	0	0.03	0	0	0	0.06	0	0	0.33	1.3
Imbalance												
H	0	0	0	0	0	0	0	0	0	0	0	0
I	0	0	0	0	0	0	0	0	0	0	0	0
I	0	0.01	0	0.01	0	0	0	0.01	0	0	0.12	2.04
L	0	0	0	0	0	0	0	0	0	0	0.06	1.08
Location	1		2		3		4		5		6	
Borin [mV - Ground #1]												
Orange	-242.1	-233.3	-276.1	-184.5	-291.1	-271.4						
Blue	-556.6	-240.6	-102.8	-98.6	-490.3	-276.7						
Black	-242.2	-233.3	-276.1	-184.5	-291.1	-271.4						
Yellow	198.0	219.9	181.4	234.3	195.2	-212.3						
Red	-556.7	-240.6	-102.8	-98.6	-490.3	-276.7						
Borin [mV - Ground #2]												
Orange	-242.1	-233.3	-276.1	-184.5	-291.1	-271.4						
Blue	-556.6	-240.6	-102.8	-98.6	-490.3	-276.7						
Black	-242.2	-233.3	-276.1	-184.5	-291.1	-271.4						
Yellow	198.0	219.9	181.4	234.3	195.2	-212.3						
Red	-556.7	-240.6	-102.8	-98.6	-490.3	-276.7						

Instrument Calibration		
	Corr	Imbal
Zero	5.07	0.03
Zero	4.99	0.03

Table B4. Sensor data after 4 months.

Month 4 Data												
Location	1		2		3		4		5		Salt Coupon	
	Corr	Imbal	Corr	Imbal								
Corrator	0.02	0	0	0	0.01	0.01	13.8	0.65	0.02	0.02	0.01	0
Location	1		4		5		FR1		FR2		Salt Coupon	
Chloride Ladders												
Corrosion	Corr	Imbal	Corr	Imbal								
H	0	0	0	0.03	0	0	0	0	0.04	0.07	0.04	0.54
I	0	0	0	0.01	0	0	0	0	0	0.01	0	0.01
L	0	0	0	0	0	0	0	0	0	0.06	0	0
Imbalance												
H	0	0	0	0	0	0	0	0	0	0	0.2	0.26
I	0	0	0	0.02	0	0	0	0	0	0	0	0
I	0	0.01	0	0	0	0	0	0	0	0	0	0
L	0	0	0	0	0	0	0	0	0	0	0	0
Location	1		2		3		4		5		6	
Borin [mV - Ground #1]												
Orange	-330.0		-313.0		-210.2		-138.9		-264.7		-242.0	
Blue	-699.6		-346.2		-197.9		-68.7		-609.0		-107.1	
Black	-33.0		-313.0		-210.2		-138.9		-264.7		-242.0	
Yellow	196.1		203.6		237.9		282.1		230.6		286.7	
Red	-699.6		-346.2		-197.9		-68.7		-609.0		-107.1	
Borin [mV - Ground #2]												
Orange	-330.0		-313.0		-210.2		-138.9		-264.7		-242.0	
Blue	-699.6		-346.2		-197.9		-68.7		-609.0		-107.1	
Black	-33.0		-313.0		-210.2		-138.9		-264.7		-242.0	
Yellow	196.1		203.6		237.9		282.1		230.6		286.7	
Red	-699.6		-346.2		-197.9		-68.7		-609.0		-107.1	
Instrument Calibration												
	Corr	Imbal										
Zero	5.07	0.03										
Zero	4.99	0.02										

Table B5. Sensor data after 7 months.

Month 7 Data												
Location	1		2		3		4		5		Salt Coupon	
	Corr	Imbal	Corr	Imbal								
Corrator	0.03	0	0.02	0.01	0.02	0	48.9	0.48	0.03	0.02	0.02	0.07

Location	1		4		5		FR1		FR2		Salt Coupon	
Chloride Ladders												
Corrosion	Corr	Imbal	Corr	Imbal								
H	0	0	0	0.06	0	0.01	0	0	0	0	0	0
I	0	0	0	0.05	0	0	0	0	0.01	0	0	0
L	0	0	0.01	0.05	0	0	0	0.01	0.03	0	0	0
Imbalance												
H	0	0	0	0.04	0	0.02	0	0	0	0	0	0
I	0	0	0	0	0	0.01	0	0	0	0	0	0
I	0	0	0	0	0	0.01	0	0	0	0	0	0
L	0	0	0	0	0	0	0	0.06	0	0	0	0

Location	1		2		3		4		5		6	
Borin [mV - Ground #1]												
Orange	-141.7		-51.1		-67.7		-66.0		-431.2		-161.2	
Blue	-81.7		13.4		-145.2		19.7		-528.6		-186.7	
Black	-141.7		-51.1		-67.7		-66.0		-431.2		-161.2	
Yellow	287.0		342.1		351.7		377.5		308.0		365.6	
Red	-81.7		13.4		-145.2		19.7		-528.6		-186.7	
Borin [mV - Ground #2]												
Orange	-141.7		-51.1		-67.7		-66.0		-431.2		-161.2	
Blue	-81.7		13.4		-145.2		19.7		-528.6		-186.7	
Black	-141.7		-51.1		-67.7		-66.0		-431.2		-161.2	
Yellow	287.0		342.1		351.7		377.5		308.0		365.6	
Red	-81.7		13.4		-145.2		19.7		-528.6		-186.7	

Instrument Calibration		
	Corr	Imbal
Zero	5.07	0.04
Zero	4.99	0.02

Table B6. Sensor data after 10 months.

Month 10 Data												
Location	1		2		3		4		5		Salt Coupon	
	Corr	Imbal	Corr	Imbal								
Corrator	0.02	0.01	0.02	0.01	0.02	0.01	0.49	0.36	0.02	0.01	0.03	0.08

Location	1		4		5		FR1		FR2		Salt Coupon	
Chloride Ladders												
Corrosion	Corr	Imbal	Corr	Imbal								
H	0	0	0	0.07	0	0	0	0	0	0	0	0
I	0	0	0	0.06	0	0	0	0	0	0	0	0.03
L	0	0	0	0.05	0	0	0	0	0	0	0	0
Imbalance												
H	0	0	0	0.04	0	0	0	0	0	0	0	0
I	0	0	0	0	0	0	0	0	0	0	0	0
I	0	0	0	0	0	0	0	0	0	0	0	0
L	0	0	0	0	0	0	0	0	0	0	0	0

Location	1		2		3		4		5		6	
Borin [mV - Ground #1]												
Orange	-10.1		0.8		98.0		-73.1		-189.2		-43.9	
Blue	-9.7		10.3		-197.0		10.4		-435.0		33.3	
Black	-10.1		0.8		98.0		-73.1		-189.2		-43.9	
Yellow	331.1		304.2		340.0		369.4		280.1		386.2	
Red	-9.7		10.3		-197.0		10.4		-435.0		33.3	
Borin [mV - Ground #2]												
Orange	-10.1		0.8		98.0		-73.1		-189.2		-43.9	
Blue	-9.7		10.3		-197.0		10.4		-435.0		33.3	
Black	-10.1		0.8		98.0		-73.1		-189.2		-43.9	
Yellow	331.1		304.2		340.0		369.4		280.1		386.2	
Red	-9.7		10.3		-197.0		10.4		-435.0		33.3	

Instrument Calibartion		
	Corr	Imbal
Zero	5.07	0.04
Zero	4.99	0.02

Table B7. Sensor data after 13 months.

Month 13 Data												
Location	1		2		3		4		5		Salt Coupon	
	Corr	Imbal	Corr	Imbal	Corr	Imbal	Corr	Imbal	Corr	Imbal	Corr	Imbal
Corrator	0	0	0.01	0	0	0	OVR	0.91	0	0	0.04	0.01
Location	1		4		5		FR1		FR2		Salt Coupon	
Chloride Ladders												
Corrosion	Corr	Imbal	Corr	Imbal	Corr	Imbal	Corr	Imbal	Corr	Imbal	Corr	Imbal
H	0	0	0	0	0	0	0	0	0	0	0	0
I	0	0	0	0	0	0	0	0	0	0	0	0
L	0	0	0	0	0	0	0	0	0	0	0	0
Imbalance												
H	0	0	0	0	0	0	0	0	0	0	0	0
I	0	0	0	0	0	0	0	0	0	0	0	0
I	0	0	0	0	0	0	0	0	0	0	0	0
L	0	0	0.01	0	0	0	0	0	0	0	0	0
Location	1		2		3		4		5		6	
Borin [mV - Ground #1]												
Orange	-187.9	-272.0	-241.3	-100.0	-410.6	-108.8						
Blue	-90.6	-104.2	-86.1	-112.1	-574.0	-120.6						
Black	-187.9	-272.0	-241.3	-100.0	-410.6	-108.8						
Yellow	25.8	186.1	246.0	315.6	185.8	325.5						
Red	-90.6	-104.2	-86.1	-112.1	-574.0	-120.6						
Borin [mV - Ground #2]												
Orange	-187.9	-272.0	-241.3	-100.0	-410.6	-108.8						
Blue	-90.6	-104.2	-86.1	-112.1	-574.0	-120.6						
Black	-187.9	-272.0	-241.3	-100.0	-410.6	-108.8						
Yellow	25.8	186.1	246.0	315.6	185.8	325.5						
Red	-90.6	-104.2	-86.1	-112.1	-574.0	-120.6						
Instrument Calibartion												
	Corr	Imbal										
Zero	5.07	0.03										
Zero	4.99	0.02										

The reference electrodes each had two, built-in steel coupons. Figure B7 shows the potentials of these coupons versus time for the six test locations. Again the noble potentials (e.g., around -0.100 mV vs. Ag/AgCl/Sat KCl) are qualitatively indicators of steel that is likely in a passive condition, while active potentials (e.g., more negative than say, -0.250 mV vs. Ag/AgCl/sat KCl) indicate higher probability of corrosion activity. The potentials and trends indicated by the reference electrode built-in coupons did not exactly match the actual steel rebar measured potentials.

Figure B8 represents a plot of the potentials of the rebar (versus Ag/AgCl/sat. KCl reference electrodes) in the steel-reinforced section of

the bridge at the six test locations. The initial noble potential values would suggest the passive condition of steel rebar in the highly alkaline (pH ~ 13) concrete environment. There was a general potential shift towards more active values over 10 months, and then a drift toward more noble potentials at 13 months. While active potentials typically suggest increased corrosion activity (i.e., possible loss of passivity at the corresponding areas), the actual corrosion rates indicated by the CORRATER LPR probes were low in all cases except at location 4, where rates appeared to increase and then decrease very dramatically.

The corrosion potentials measured with respect to the reference electrodes indicated corrosion activity ranging from passive to active behavior. However, very low corrosion rates were indicated by the corrosion rate sensors, typically less than 0.1 mpy and with very low pitting propensity. The primary reason for this observation is that insufficient chloride has migrated through the concrete bridge deck to stimulate detectable corrosion attack during the 13-month study. This is not surprising because it takes many years, and often, decades, for a significant amount of chloride to permeate through good quality concrete; a thicker concrete cover also impedes chloride migration. (See Figures B7 and B8).

The concrete test block salt coupon artificially contaminated with chloride indicated generally greater corrosion activity at 1 and 4 months compared to the bridge deck. However, this activity diminished at 7, 10, and 13 months, probably due to drying out of the test block. (Figure B9).

Corrosion will eventually be detected when enough chloride has reached the sensors embedded in the bridge deck concrete. The greater the amounts and frequency of deicing road salt usage, the shorter the chloride permeation time leading to significant corrosion. Even then, it could take many years. Therefore, it is recommended that monitoring of the corrosion sensors embedded in the concrete bridge deck at Fort Knox be continued (for example every 5 years), to confirm their veracity.

Figure B7. Coupon potentials vs. time at the six test locations on the steel-reinforced section of the bridge.

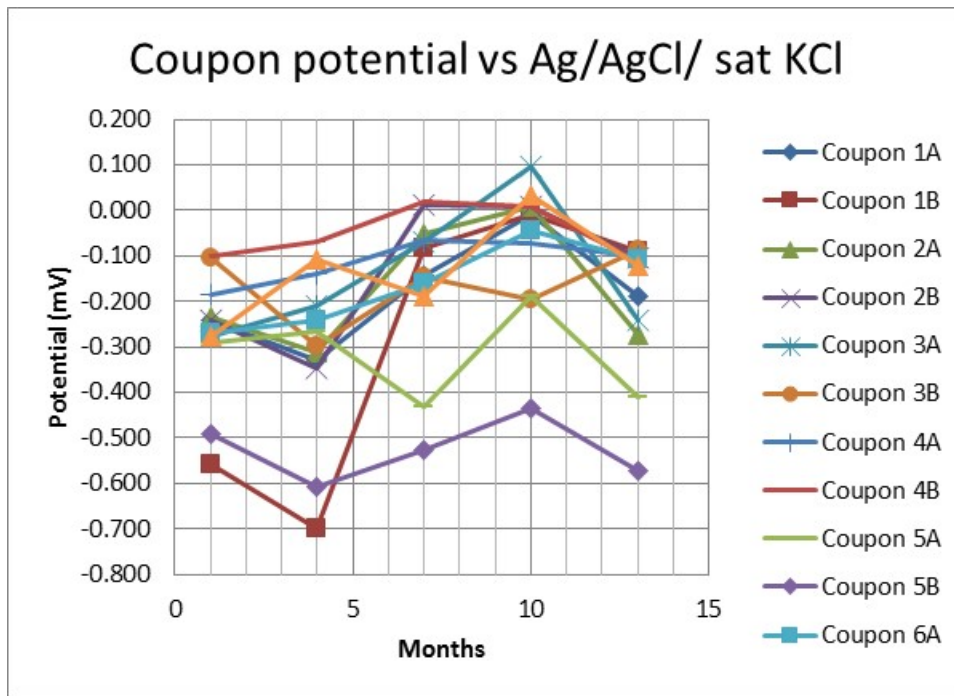


Figure B8. Rebar potential vs. time at the six test locations on the steel-reinforced section of the bridge.

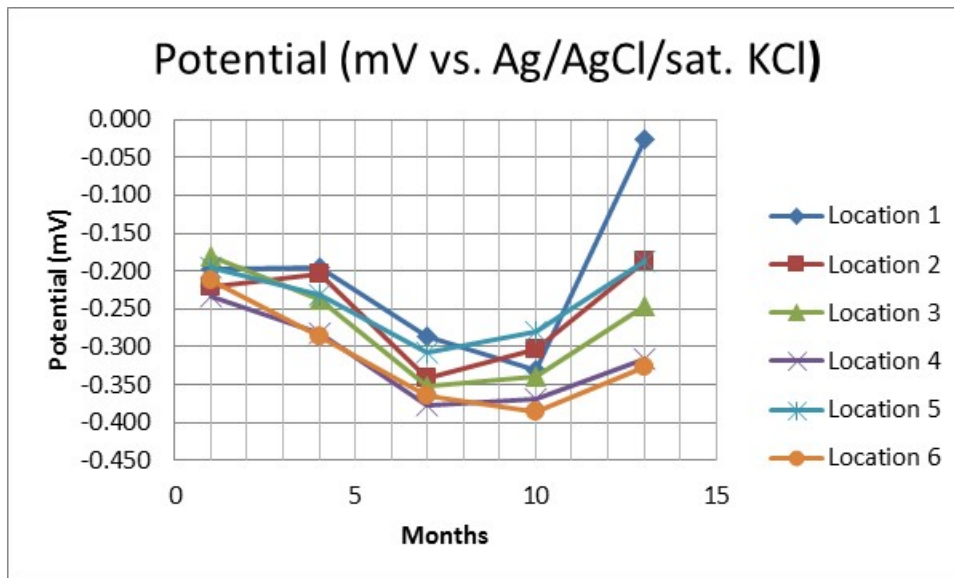
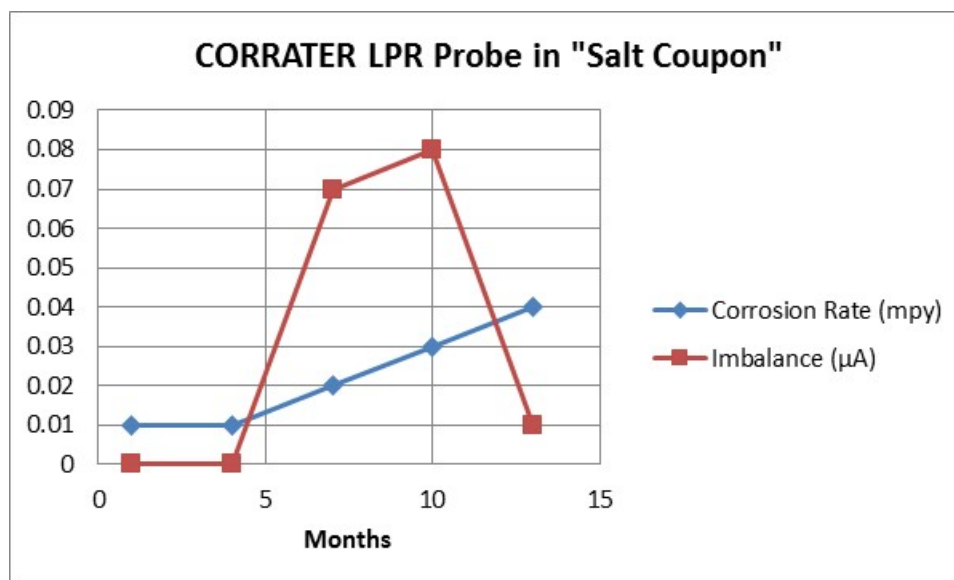


Figure B9. Corrosion rate and imbalance readings vs. time for CORRATER probe in artificially-contaminated concrete block "salt coupon."



Corrosion coupon rack assessment

The atmospheric corrosion coupon rack placed at the site had coupons removed at 6 and 12 months. These coupons were sent to a certified lab and mass loss was measured per ASTM G1-03 on the AL 6061 T6, AL 2024 T3, AL 7075 T6, C 1010, and CDA 101. The silver test coupon had Coulometric Reduction of Surface Films done per ASTM B 825-13. These test results are included as Attachments 1 and 2 at the end of this appendix. A summary of the results and classification according to the categories listed in Table 2 from ISO 9223:2012 are shown in Table 2 and Table 3 in Section 3.1.1 of this report. The copper experienced a high mass loss in comparison to the other metals. The results from the 12-month testing suggest that the 2024 and 7075 aluminum alloys experienced an extremely high mass loss due to corrosion. These results are inconsistent with the other alloys and the results from the weather data analysis; therefore, the mass loss test from the 12 month 7075 and 2024 coupon have been omitted from the atmospheric corrosion severity classification of the site.

Corrosion severity site classification

The results from the ISO 9223:2012 analysis of weather data and mass loss testing suggest the Fort Knox Bridge #4 site is a Category 3 classification of atmospheric corrosion severity. Although the steel coupon testing resulted in a Category 2 classification, the results were on the upper limit of

the category. The potential for corrosion at the site is considered medium. The corrosion sensors show no corrosion in the bridge and validate this classification as being much less than severe.

Attachment 1



1049 Triad Court, Marietta, Georgia 30062 • (770) 423-1400 Fax (770) 424-6415

ACCELERATED ENVIRONMENTAL TEST REPORT					
Ref. D201577		Date November 29, 2013		Page 1	of 2
Christopher Olaes Mandree Enterprise Corp. 812 Park Dr. Warner Robins, Georgia 31088			Purchase Order #: 2012-22		
Procedure					
<u>Test Performed</u> Mass Loss Evaluation			<u>Method</u> ASTM G1-03 (2011)		
<u>Test Material</u> Metal Test Coupons			<u>Requirements</u> None Specified		
Results					
Sample ID	Part Number	Initial Weight [g]	Final Weight [g]	Δ Weight [g]	Weight Loss %
AL6061 T6	COR123400304100	9.30895	9.30359	0.00536	0.06
AL2024 T3	COR122990304100	8.98105	8.97847	0.00258	0.03
AL7075 T6	COR123470304100	9.36348	9.35870	0.00478	0.05
CDA1010	COR124140304100	32.60544	32.50175	0.10369	0.32
CDA101	COR124140304100	28.64740	28.23034	0.41706	1.46



Prepared by: F. Lopez
F. Lopez
Supervisor

Approved by: E. W. Sproat
E. W. Sproat
Group Manager

This report may not be reproduced except in full without the written approval of ATS. This report represents interpretation of the results obtained from the test specimen and is not to be construed as a guarantee or warranty of the condition of the entire material lot. If the method used is a customer provided, non-standard test method, ATS does not assume responsibility for validation of the method.



APPLIED TECHNICAL SERVICES, INCORPORATED

1049 Triad Court, Marietta, Georgia 30062 • (770) 423-1400 Fax (770) 424-6415

ACCELERATED ENVIRONMENTAL TEST REPORT		
Ref. D201577	Date November 29, 2013	Page 2 of 2
Christopher Olaes Mandree Enterprise Corp. 812 Park Dr. Warner Robins, Georgia 31088		Purchase Order #: 2012-22
Procedure		
<u>Test Performed</u> Coulometric Reduction of Surface Films on Metallic Surfaces		<u>Method</u> ASTM B 825-13
<u>Test Material</u> Silver Test Coupon		<u>Requirements</u> None Specified
Results		
Sample ID	Part Number	Results
Ag	COR117520304100	Reduction Time = 1025 Seconds Total Reduction Charge = 1.943 Coulombs



Prepared by: F. Lopez F. Lopez
Supervisor

Approved by: Gene Price Gene Price, P.E.
Senior Engineer

This report may not be reproduced except in full without the written approval of ATS. This report represents interpretation of the results obtained from the test specimen and is not to be construed as a guarantee or warranty of the condition of the entire material lot. If the method used is a customer provided, non-standard test method, ATS does not assume responsibility for validation of the method.

Attachment 2



1049 Triad Court, Marietta, Georgia 30062 • (770) 423-1400 Fax (770) 424-6415

MATERIALS TEST REPORT					
Ref. D209559	Date February 18, 2014	Page 1	of 7		
Christopher Olaes Mandaree Enterprise Corp. 812 Park Dr. Warner Robins, Georgia 31088			Purchase Order #: 2012-22		
Procedure					
<u>Test Performed</u> Mass Loss Evaluation			<u>Method</u> ASTM G1-03 (2011)		
<u>Test Material</u> Metal Test Coupons			<u>Requirements</u> None Specified		
Results					
Sample ID	Part Number	Initial Weight [g]	Final Weight [g]	Δ Weight [g]	Weight Loss %
AL6061 T6	COR123400304100	9.5998	9.5940	0.00536	0.06
AL2024 T3	COR122990304100	9.1249	8.8314	0.00258	0.03
AL7075 T6	COR123470304100	9.6156	9.4233	0.00478	0.05
C1010	COR124140304100	28.5495	27.5658	0.10369	0.32
CDA101	COR124140304100	32.3241	32.1816	0.41706	1.46

ISO 9001

Prepared by: _____ T. Burris
Materials Testing

Approved by: _____ F. Lopez
Supervisor

This report may not be reproduced except in full without the written approval of ATS. This report represents interpretation of the results obtained from the test specimen and is not to be construed as a guarantee or warranty of the condition of the entire material lot. If the method used is a customer provided, non-standard test method, ATS does not assume responsibility for validation of the method.

ATS APPLIED TECHNICAL SERVICES, INCORPORATED

1049 Triad Court, Marietta, Georgia 30062 • (770) 423-1400 Fax (770) 424-6415

MATERIALS TEST REPORT			
Ref.	D209559	Date	February 18, 2014
Page	2	of	7



Figure 1: AL6061 T6 Sample prior to Corrosion Removal



Figure 2: AL6061 T6 after Corrosion Removal

ATS APPLIED TECHNICAL SERVICES, INCORPORATED

1049 Triad Court, Marietta, Georgia 30062 • (770) 423-1400 Fax (770) 424-6415

ACCELERATED ENVIRONMENTAL TEST REPORT			
Ref.	D209559	Date	February 18, 2014
Page	3	of	7



Figure 3: AL2024 T3 Sample prior to Corrosion Removal



Figure 4: AL2024 T3 after Corrosion Removal

ATS APPLIED TECHNICAL SERVICES, INCORPORATED

1049 Triad Court, Marietta, Georgia 30062 • (770) 423-1400 Fax (770) 424-6415

ACCELERATED ENVIRONMENTAL TEST REPORT			
Ref. D209559	Date February 18, 2014	Page 4	of 7



Figure 5: AL7075 T6 Sample prior to Corrosion Removal



Figure 6: AL7075 T6 after Corrosion Removal

ATS APPLIED TECHNICAL SERVICES, INCORPORATED

1049 Triad Court, Marietta, Georgia 30062 • (770) 423-1400 Fax (770) 424-6415

ACCELERATED ENVIRONMENTAL TEST REPORT			
Ref. D209559	Date February 18, 2014	Page 5	of 7



Figure 7: C1010 Sample prior to Corrosion Removal



Figure 8: C1010 after Corrosion Removal

ATS APPLIED TECHNICAL SERVICES, INCORPORATED

1049 Triad Court, Marietta, Georgia 30062 • (770) 423-1400 Fax (770) 424-6415

ACCELERATED ENVIRONMENTAL TEST REPORT			
Ref. D209559	Date February 18, 2014	Page 6	of 7



Figure 9: CDA101 Sample prior to Corrosion Removal



Figure 10: CDA101 after Corrosion Removal



APPLIED TECHNICAL SERVICES, INCORPORATED

1049 Triad Court, Marietta, Georgia 30062 • (770) 423-1400 Fax (770) 424-6415

MATERIALS TEST REPORT		
Ref. D209559	Date February 18, 2014	Page 7 of 7
Christopher Olaes Mandaree Enterprise Corp. 812 Park Dr. Warner Robins, Georgia 31088		Purchase Order #: 2012-22
Procedure		
<u>Test Performed</u> Coulometric Reduction of Surface Films on Metallic Surfaces		<u>Method</u> ASTM B 825-13
<u>Test Material</u> Silver Test Coupon		<u>Requirements</u> None Specified
Results		
Sample ID	Part Number	Results
Ag	COR117520304100	Reduction Time = 1,660 Seconds Total Reduction Charge = 3.146 Coulombs



Prepared by: _____ F. Lopez
Supervisor

Approved by: _____ Gene Price, P.E.
Senior Engineer

This report may not be reproduced except in full without the written approval of ATS. This report represents interpretation of the results obtained from the test specimen and is not to be construed as a guarantee or warranty of the condition of the entire material lot. If the method used is a customer provided, non-standard test method, ATS does not assume responsibility for validation of the method.

Appendix C: Excerpts from Hybrid-Composite Beam (HCB®) Design and Maintenance Manual

The following pages are excerpts from a report prepared for the Missouri Department of Transportation for a bridge in Missouri (Hillman 2012). While the report was not prepared for the bridge section that is the subject of this report, the report's selected pages provide valuable information for the design, inspection, and maintenance of hybrid composite beams.

The full report can be accessed at aii.transportation.org/Documents/BMDQ/HCB-design-maint-manual.pdf.

1.0 INTRODUCTION AND GENERAL PRINCIPALS

1.1 THE HYBRID-COMPOSITE BEAM (HCB®)

Considerable work has been done since the late 1980's to the present day with respect to Fiber Reinforced Polymer or FRP elements for transportation infrastructure applications. In order to emphasize the unique characteristics of the HCB, it is important to point out that most of the research in advanced composite materials for transportation applications has been limited to structural shapes comprised of homogeneous FRP materials. Other research includes the application of FRP materials to conventional structural members to enhance strength and serviceability. The following is a non-exhaustive list of the various FRP research categories with respect to the bridge industry:

- Bridge framing systems using glass FRP beams or trusses manufactured from pultruded shapes.
- Glass FRP cable stayed pedestrian bridges fabricated from pultruded shapes with FRP cable stays.
- FRP reinforcing bars and post-tensioning strand for reinforcing and prestressing conventional concrete beams.
- Bonding FRP sheets to existing concrete and steel structures as a means of repairing, strengthening and upgrading these structures.
- FRP column wraps to provide confinement for enhanced seismic performance of concrete columns.
- Concrete filled, circular FRP tubes as an alternate to reinforced concrete columns.
- FRP bridge decks manufactured as pultruded sections, or VARTM sandwich panels.
- Hybrid pultruded beams using carbon reinforced flanges and glass-reinforced webs.

In most cases, where bridges have been constructed of structural members fabricated entirely of FRP, these bridges are subject to constraints that have precluded widespread acceptance of the technology. First and foremost has been cost. The increased costs can be directly traced to raw material costs and inefficiencies due to constitutive material properties. In general, both glass and carbon have a strength capacity that meets or greatly exceeds that of steel. However, these materials are much more flexible and typically require additional material beyond what is required for strength to satisfy the serviceability requirements for deflections. The amount of material required for deflection control coupled with the higher material costs have traditionally made it more difficult for a purely FRP beam to be cost competitive with concrete or steel beams.

Other limitations in application and span length constraints for FRP beams have resulted from lower shear strength capacity and low elastic buckling capacity in compression. Combined with the flexible nature of these materials, applications of purely FRP bridges have generally been confined to pedestrian bridges and short span county bridges. Although the increased service life can improve the life cycle costs, FRP structures built in the early years of development were seldom, if ever, cost effective on a first cost basis.

What distinguishes the HCB from some of the earlier FRP structures is that it uses conventional materials, i.e. concrete and steel, in conjunction with FRP components to create a structural member that exploits the inherent benefits of each material in such a manner as to optimize the overall performance of the combination of materials. Whereas FRP materials are generally too expensive and too flexible when arranged in a homogeneous form, the strength and stiffness in the HCB are provided by a more efficient use of materials that are well suited to purely axial tension or compression. The classical arch shape of the compression reinforcing also helps reduce the shear carried by the FRP webs and ensures an optimal use of the compression and tension reinforcing. The culmination is a composite beam system that provides lighter weight for transportation and erection with enhanced corrosion resistance that can be cost competitive with conventional materials on a first cost basis.

In its most general form, the HCB is comprised of three main sub-components that are the shell, compression reinforcement and tension reinforcement. The first of these is the FRP beam shell, which encapsulates the other two sub-components. The second major sub-component is the compression reinforcement which consists of portland cement grout or concrete which is pumped or pressure injected into a continuous conduit fabricated into the beam shell. The third and final major sub-component of the beam is the tension reinforcement, which is used to equilibrate the internal forces in the compression reinforcing. This tension reinforcing could consist of unidirectional carbon or glass fibers or it could consist of steel fibers, e.g., standard mild reinforcing steel or prestressing strand infused in the same matrix during fabrication of the glass beam shell. The orientations of these sub-components are graphically displayed in Figure 1.1. As a result of the orientation of the materials, the concrete, for the most part is in pure compression. The steel is in pure tension. As noted previously the arch profile of the compression reinforcement allows for much of the shear to be carried by the concrete.

Bridge B0439

HCB-Maintenance Manual

August 2012

Subsequently, the FRP webs of the beam can be made relatively thin, resulting in a more efficient use of the FRP in the shell.

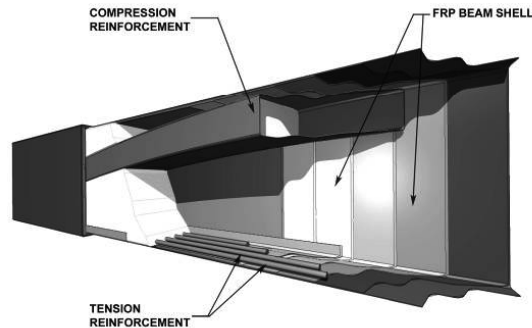


FIGURE 1.1 - Fragmentary Perspective of Hybrid-Composite Beam

Despite the unique configuration and diverse nature of the building materials used in the HCB, the end product does not result in any unique characteristics that preclude the beam from being used in the same manner as more conventional framing systems. The cross-section is very conducive to standardization, similar to prestressed beams or rolled steel sections. Yet at the same time the tooling required for the Vacuum Assisted Resin Transfer Molding (VARTM) manufacturing process is simplistic and inexpensive and allows for considerable variation with respect to overall dimensions, shape and internal lay-up. The embodiment of the HCB results in a beam that has several inherently unique benefits, while remaining cost competitive with conventional materials.

The beam shell is constructed of a vinyl ester resin reinforced by glass fibers optimally oriented to resist the anticipated forces in the beam. The beam shell includes a top flange, bottom flange and a continuous conduit. The conduit is fabricated into the shell and runs longitudinally and continuously between the ends of the beam along an arch profile that is designed to conform to the internal load path resisting the external forces applied to the beam. The beam shell also includes two vertical webs, which serve to transfer the applied loads to the composite beam as well as to transfer the shear forces between the compression reinforcement and tension reinforcement. All of the components of the beam shell are fabricated monolithically using the VARTM process.

The compression reinforcement, which typically consists of self-consolidating concrete (SCC), is pumped into the conduit within the beam shell through the ports located at the centerline and ends of the beams (depending on the lengths of the beams, there may be additional ports at 15 to 20 foot spacing). The profile of the compression reinforcement follows a parabolic profile which starts at the bottom corners of the beam ends and reaches an apex at the center of the beam such that the conduit is tangent to the top flange. The profile of the compression reinforcement is designed to resist the compression and shear forces resulting from vertical loads applied to the beam in much the same manner as an arch structure.

The thrust resisted by the compression reinforcement resulting from externally applied loads is equilibrated by the tension reinforcement. The tension reinforcement consists of layers of unidirectional steel reinforcing fibers with a high tensile strength and high elastic modulus. The fibers, which are located just above the glass reinforcing of the bottom flange, are oriented along the longitudinal axis of the hybrid-composite beam. The tension reinforcement is fabricated monolithically into the composite beam at the same time the beam shell is constructed. Subsequently, the strands are completely encapsulated in the same resin matrix as the glass fabrics. The most common type of tension reinforcing used today in HCB's is 270 ksi, galvanized, prestressing strand.

A bridge can be built quickly and easily using the HCB. The beams are typically erected prior to injection of the compression reinforcement by placing them with a crane in the same manner as a steel or prestressed concrete beam. The composite beams are easily self-supporting prior to and during the installation of the compression reinforcement. In the case of bridge replacement or rehabilitation it may be possible to reuse existing abutments and/or intermediate piers. The compression reinforcement is then introduced into the composite beam by placing the portland cement concrete into the profiled conduit in the FRP beam shell. No temporary falsework is required for the erection of the composite beams or during the installation of

Bridge B0439

HCB-Maintenance Manual

August 2012

the compression reinforcing. For some applications, such as railroad bridges, it may be desirable to cast the compression reinforcing prior to shipping the beams to the project site. This was the case in the prototype bridge first installed on the railroad test track. Although a railroad bridge constructed using HCB can still be less than half the weight of a concrete bridge, speed of installation for railroad bridge construction is generally more important than extreme lightweight.

There are also cases where the arch concrete will be placed prior to erection of the HCB's, but the concrete deck is still cast-in-place. Any time portions of the concrete are precast prior to erection, the pick points for the beam become more sensitive. With the empty shell, the beams can be picked from almost any location. Once the concrete arches are cast, it is important to lift the beams from the ends to avoid introducing tension stresses in the arch concrete. In most cases, strand lifting loops or other lifting inserts are placed in the chimneys at the ends of the beam prior to arch casting, to provide the requisite lifting devices.

For most typical applications, the weight of the HCB during transportation and erection is approximately one fifth of the weight of the conventional steel beam required for the same span and approximately one tenth of the weight required for a precast prestressed concrete beam for the same span. This light weight coupled with the corrosion resistant nature of the FRP materials make this technology well suited to "Accelerated Bridge Construction" and for providing bridges with service lives that should exceed one hundred years.

2.0 STRUCTURAL DESIGN AND ANALYSIS

In order to assess the limit states that are required to quantify the behavior of the hybrid-composite beam system, it is worth briefly considering the general evolution of structures through the course of time. Some of the first structures ever contrived were stone arches. Without any calculations at all, it became evident that by placing blocks of stone sequentially in a circular curve, it was possible to create a structure that would span a distance equal to the diameter of the circle. Centuries later, with the advent of materials such as iron and steel, it became possible to span greater distances with much lighter structures. As the steel rolling mills and fabrication technology became more sophisticated, complex riveted trusses gave way to sleek rolled sections and welded plate girders.

Engineers continued to experiment with hybrid structures, utilizing more than one type of building material to comprise a structural member. One of the most simplistic concepts in the history of structural engineering, which is now completely taken for granted, is the concept of adding reinforcing steel to a concrete beam to dramatically increase the load carrying capacity of the member. Nowadays, we simply refer to these as concrete beams. However in actuality they are really hybrid-composite structures, relying on a more optimized utilization of two very different materials.

In almost every instance, as engineers create new structural forms, it is necessary to develop a methodology for quantifying the behavior of the various materials within the specific embodiment intended. Such is the case with the evolution of fiber-reinforced polymers (FRP). In general, various methods of structural analysis that evolved for other types of materials can also be applied to the analysis and design of FRP structures. Certainly statics is applicable. The theory of elasticity and general mechanics of materials also remain essentially unchanged, particularly as they apply to conventional materials such as steel.

There are two fundamental assumptions that differentiate FRP structures from steel structures. One difference is that steel is assumed to be elastic, perfectly plastic. In other words, the stress strain relationship for this material can be accurately represented with a bifurcated, bilinear curve. This property also allows the steel to undergo a significant increase in strain after reaching its yield strength and prior to a brittle rupture. The other property of steel that grossly simplifies analysis and design is that it is an isotropic material. In other words, it has essentially the same constitutive properties in all directions.

In contrast to steel, FRP materials generally remain linearly elastic up to the point of a brittle failure mode. To further complicate analysis, FRP structural components are anisotropic rather than isotropic. In other words, the constitutive properties of these materials can vary in each direction, and are a function of the specific composition of the material. In the case of glass fiber reinforced composites and carbon fiber reinforced composites, the strength and stiffness properties are typically a function of the fiber volume ratios and the specific orientation of the fibers. Because of these fundamental differences, FRP structures require additional consideration in design and analysis. An in depth derivation of the theory of elasticity for non-linear, non-isotropic material behavior is beyond the scope of this project. However, this information is available in numerous texts and will be elaborated on where it is necessary to evaluate certain limit states. One generalization that can be made is that, based on the development to date, it is not evident that a rigorous analysis of the FRP materials is warranted to arrive at a safe and functional design.

Computational Development: By definition, the HCB is comprised of several different materials. Each component of the beam serves at least one specific structural purpose. The concept behind the HCB is to select materials that are well suited to satisfying particular design limit states, and arranging them in such a manner as to optimize the structural behavior of the overall beam. In general terms the HCB is comprised of three main sub-components that are the shell, the compression reinforcement and the tension reinforcement. With regard to some limit states, the HCB behaves similar to a reinforced concrete beam. In some respects, it behaves similar to a steel box beam. Finally, with respect to many of the limit states, the FRP components do contribute to the resistance. As a result, some additional consideration has to be given to the analysis of these components of the structure.

One of the primary goals in developing an efficient design for any structure is to determine a predictable mode of failure and attempt to provide an optimized design for all of the limit states such that the intended failure mode will still govern. It was not evident in the early stages of HCB development, how each limit state would be quantified, or how the behavior of each different component of the beam would influence the design. Because of this lack of intuitive knowledge, the development of a design spreadsheet was initiated that would provide a means of investigating the limit states simultaneously to facilitate quick preliminary designs. Subsequently, these design tools make it possible to

Bridge B0439

HCB-Maintenance Manual

August 2012

investigate the impacts to all limit states, as modifications are made to a specific component and perform parametric studies to converge on more efficient designs.

The following sections of this report will provide a more detailed discussion of the more critical design limit states considered in the development of the HCB. This information can serve as a guide in performing and/or reviewing design calculations for a specific bridge. The following list identifies how the design is compartmentalized to facilitate book keeping during design:

- INPUT
- SECTION
- DESIGN LOADS
- SHEAR
- DEFLECTIONS
- BENDING (NON-COMPOSITE)
- BENDING (COMPOSITE)
- BENDING (NEGATIVE MOMENTS)
- STRESSES (POSITIVE BENDING)
- STRESSES (NEGATIVE BENDING)

The initial design spreadsheet compiled includes a live load generator for calculation of simple span moments for:

- HS-20 (Lane and Truck Loads for AASHTO Standard Specifications)
- HL-93 (Lane and Truck Loads for AASHTO LRFD Specification)
- Cooper E-80 (Locomotive and Alternate Load for AREMA Specifications)
- Uniform Live Load (For building applications or alternate pedestrian loads on bridges)

Where bridges are designed to be continuous for live loads, a separate live load generator is suggested. The current design spreadsheet tools have been set-up for post-processing once the design live load forces have been calculated at 1/10th points along the beams. Other types of live loads can be evaluated as well, but the designers are cautioned to pay special attention to the bookkeeping, as the HCB does not have prismatic section properties.

INPUT: The INPUT section of the design calculations is primarily to establish the bridge geometrics, the constitutive properties for the various materials, the governing code for evaluation and any corresponding unit weights or loads that need to be evaluated based on the structure type. Regarding unit weights and loads, this applies primarily to dead load and superimposed dead loads such as parapets, future wearing surfaces, ballast, rails, etc. For the most part, this input information is specific to a bridge project and not unique to the HCB, with the exception of some of the constitutive properties of the FRP materials.

SECTION: In order to perform the serviceability and strength capacity checks for the HCB, it is necessary to define the exact section under consideration. The information specific to the geometry of the HCB is input in SECTION. This information is used to define the cross-section of the HCB and calculate the section properties. Demonstrated in Figure 2.1 is a generalized beam cross-section showing both steel tension reinforcing and supplemental fiber tension reinforcing, which could be carbon or additional glass fabric.

Due to the isotropic nature of steel, it is possible with steel structural members to calculate the area and inertia of the cross-section without consideration of the elastic modulus. In calculating the section properties of the HCB, it is necessary to consider the relative constitutive properties of the various materials used. As a result it is necessary to select the elastic modulus of one material to serve as the basic value to be used in analysis. In the case of the HCB, it was determined that a logical choice for the base material would be the glass FRP webs. The primary reason being that this is the material most likely to remain relatively constant whereas the material selected for the compression and tension reinforcing could result in dramatically different elastic moduli. Further, the elastic modulus of concrete is not well suited as a constant, in that as concrete approaches its ultimate strain, the material cannot be accurately represented with a constant value for the elastic modulus.

By selecting one material as the reference, all of the other materials comprising the beam are then transformed into equivalent areas of this same material using the respective modular ratios "n". As a result, the modular ratio used for transforming steel tension reinforcing to an equivalent amount of FRP would be $n_s = E_{\text{steel}}/E_{\text{web}}$ and likewise for the other

Bridge B0439

HCB-Maintenance Manual

August 2012

materials. The modulus of elasticity assumed for the laminate is typically based on the constitutive properties acquired from ASTM tests on witness panels made during the fabrication of previous beams. The properties can also be calculated using equations based on the rules of mixture of the glass and resin components as is common in the composite industry. However the test data yields more accurate results and has historically provided excellent accuracy in calculating the predicted deflections. It should be noted that for all intents and purposes, the foam component is ignored in the calculations. Although the foam is neglected in calculations, it does serve several important purposes that will be discussed in more detail later.

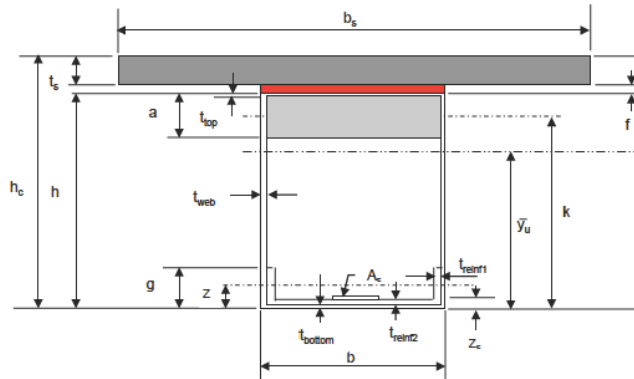


Figure 2.1 - Typical Cross-Section Geometry

In calculating the cross sectional properties for the HCB, it is important to remember that due to the profile of the compression reinforcement, the section properties are not prismatic along the length of a beam. As a result, the section properties are calculated at 1/10th points along the beam based on a parabolic profile of the compression arch. Due to the construction sequencing of the HCB, it is also necessary to calculate separate properties for the HCB shell by itself, the HCB shell acting compositely with the concrete arch and the full composite properties of the HCB with the arch concrete and the composite concrete deck.

Once all of the geometric data and constitutive properties of the materials have been input, the cross-sectional areas and moments of inertia can be tabulated for the beam under consideration. It is also at this time that the self-weight of the structural member is calculated, both with and without the compression reinforcing in place. The calculated properties of the section are then used in subsequent calculations to help design the components of the beam for the various design limit states.

DESIGN LOADS: The design loads for consideration on the bridge are typically governed by specific codes. In the USA these codes generally include the American Railway Engineering and Maintenance-of-Way Association (AREMA), Manual for Railway Engineering, and for highways, the American Association of State Highway Transportation Officials (AASHTO) LRFD Bridge Design Specifications. Ultimately the owner usually dictates the governing loads for design of a bridge. The following is a brief description of the book keeping procedures necessary to compile the design forces and allow the designer to tailor the calculations to a specific application.

Bridge Geometrics and Composition: In this section, the designer must define the cross section of the overall structure to be considered. In most bridge designs, it is acceptable to distribute superimposed dead loads uniformly to all of the beams in a cross section. As a result, in defining the cross-section, the designer must identify all of the superimposed dead loads to be applied to the cross-section. Some of the information in this section might include:

- Span Length
- Deck Width
- Depth of Ballast

Bridge B0439

HCB-Maintenance Manual

August 2012

- Slab Thickness
- Parapet Loads
- Overlay Thickness and Weight
- Rail Loads

Dead Loads: Once the number of girders to be included in the overall cross-section of the structure as well as the girder spacing has been selected the dead loads per unit length of beam can be calculated.

Superimposed Dead Loads: In many cases, portions of the dead loads on a structure may be placed or removed at a later time within the life of the structure. As a result, most design codes require that these loads be tracked separately than the basic dead loads. Superimposed dead loads typically include items such as parapets, overlays, future wearing surfaces, ballast, or in the case of buildings it could include items such as interior partitions.

Live Loads: The design live loads can vary dramatically depending on the specific application of the structure. For Class 1 Railroad bridges, live loads typically consist of the Cooper E-80 Load or the Alternative Live Load as specified in AREMA. For highway bridges, the design load considered is the HL-93 load as specified by AASHTO. For building loads, the designer must input a uniformly distributed pressure. The information provided previously, including the number of girders and the beam spacing are used to calculate the distribution of live loads to the specific beam under consideration. The span length previously entered is used to determine the impact factors to be applied to live loads for highway and railroad bridges.

As noted before, the tool developed for preliminary designs does include a live load generator that is sufficient for simply supported single spans under conventional AASHTO and AREMA loads. When girders are to be designed as continuous structures, the design forces should be calculated from a more rigorous analysis and input into the design program manually. It is expected that in the near future, commercial grade software will be available that includes a more generic live load generator that works for continuous structures as well as simple spans.

Maximum Design Forces: Once all of the dead, superimposed dead and live load forces have been determined for a specific beam, these forces are compiled and combined to calculate the controlling forces for the limit states of shear and bending. The unfactored loads are considered service loads. The factored loads are also calculated using the designated load factors to be considered in ultimate strength design for various load combinations as specified in the governing design codes for the respective bridges. Primary differences between applications such as railroad bridges and highway bridges are in externally applied loads, beam spacing relative to structural cross-section, safety factors and load and resistance factors.

There are various different classifications of limit states that are applicable to structural analysis and design. HCB design considers both strength and serviceability limit states. Strength limit states are typically those that must be satisfied in order to ensure the safe performance of a structure. Serviceability limit states are those that are generally evaluated based on subjective criteria relative to an acceptable level of performance, as determined by the user, relative to a specific behavior of the structure, e.g. deflections or vibrations. It should be noted that with greater optimization of strength limit states for a structure, the controlling design criteria of serviceability limit states could become less prevalent. This is often typical of lightweight structures and has also been evident through the development of FRP structures utilized in civil applications.

Before progressing into the specifics of the various limit states, it is worth briefly mentioning the differences between the two design philosophies that are typically used with respect to structures of all types. One philosophy is typically known as working stress design (WSD) or allowable stress design (ASD). In this system, the loads applied to a structure are intended to represent forces with magnitudes that represent a realistic occurrence. The stresses in the structural members are then calculated from these realistic loads and compared to an allowable stress based on a failure stress, such as yielding of the material, divided by some factor of safety.

The second design philosophy is sometimes referred to as ultimate strength design (USD). Another terminology used is load and resistance factor design (LRFD). In this system, the design codes typically use the same service loads as in WSD, however, these loads are then amplified by load factors. The stresses, or more appropriately, the internal forces resisting the applied loads in the structural members are calculated to resist these factored loads. The ultimate capacity of

the section is calculated based on some limiting parameter such as yield strength, ultimate strength, limiting strain or elastic buckling strength of the material multiplied by some resistance factor that is generally less than 1. If the response of the structures is such that the ultimate capacity of the section is found to be greater than the factored demand on the section, then the specific design limit state under consideration is satisfied. Again, a comprehensive discussion of LRFD is beyond the scope of this manual and is available in great detail in other texts.

It is generally preferable to select one design philosophy or the other and remain consistent throughout the design and analysis of a structure. In some cases there is a duplicative evaluation of a design limit state using both philosophies. One instance of this is in the design of prestressed concrete beams where it is common to design according to some pre-determined allowable stresses for the materials (ASD), but still check the ultimate capacity of the beam using LRFD. For the HCB a reverse approach is taken, where the strength checks are performed using an LRFD approach, but the stresses under service conditions are also checked to make sure the structure is safe under each stage of construction and service. This will be addressed in more detail in subsequent sections of this manual.

Based on bridges designed and constructed to date, the structural behavior of the HCB consistently indicates that serviceability and more specifically, live load deflections govern the design. The following is a brief listing of the steps used in making decisions regarding the composition of the beam to arrive at a satisfactory design. More specific descriptions of each limit state will be discussed in more detail later.

- Establish geometrics of structural cross section.
- Make initial assumption regarding depth of girders. For railroad bridges this is typically span/10 to span/12. For highway bridges, the optimum range is span/18 to span/25.
- Make initial assumption of girder width based on depth (generally depth/3 to depth/2). Typical width of 24 inches is driven by efficient use of foam core that has standard widths of 24 inches. A single block of foam is desirable in the bottom of the beam and by using common off-the-shelf dimensions, then there is no waste of the material.
- Make preliminary assumption on thickness for FRP web and flange components. Common web thicknesses are two layers of Q64 fabric or one layer of Q102 fabric combined with a layer of X24 (these will be explained in more detail later). Either way a typical laminate thickness on the shell is on the order of 0.15 inches.
- Adjust dimensions of compression conduit and amount of tension reinforcing until deflection criteria are met. Typical dimensions of the compression arch might be 1/6 to 1/5 of the depth of the shell. The most effective ways to reduce deflections are increasing the depth of the beam and adding tension reinforcing to the bottom flange.
- Check the ultimate moment capacity of the shell and arch during placement of the deck concrete (neglecting composite action with the deck).
- Check the ultimate moment capacity of the HCB acting compositely with the deck to make sure strength is satisfied for full dead plus live loads. Adjust compression and tension reinforcing as required, although typically the use of high-strength prestressing strand results in residual capacity beyond the factored demand in the codes.
- For structures made continuous for live loads, it is also necessary to check the ultimate bending capacity over the piers. At centerline of the piers, this capacity is typically limited to the tension reinforcing in the deck and the compression block available in the HCB arch.
- Check ultimate shear capacity at 1/10th points along the beam. Increase web thickness if necessary.
- It is also important to check the positive moment stresses in each component of the beam due to bending under service level loads. In the case of continuity the negative moment bending stresses must also be checked.

This is by no means a comprehensive list of the steps necessary to design an HCB Bridge, but the steps shown are intended to serve as a guideline to performing a design. It is also intended to provide some historical background to explain where specific dimensions on an HCB may have come from when looking at future structural evaluations and load ratings.

2.1 LIMIT STATES METHODOLOGY

As is the case for the design of conventional concrete and steel structures, the design philosophy and limit states for the HCB will continue to evolve with further research. A logical argument can be made regarding the use of load and resistance factor (LRFD) design philosophy based on the prevalence of this philosophy in current structural design codes worldwide. At the same time, serviceability limit states, such as deflections, should be evaluated with unfactored loads, which is standard practice for most structures. Also like steel and concrete, the limit states for shear are much more complex and in some cases may require both ASD and LRFD checks for the HCB. It should be noted that when evaluating the performance of FRP materials, it is not unusual to use limiting strains rather than limiting stresses, as is typically done for steel and concrete structures. This will be discussed in more detail in the bending limit state check.

As noted previously, most structural design codes now use an LRFD format. As part of future development for code provisions, reliability analyses should be conducted for each limit state with respect to the statistical probability of the demand and capacity of the beam based on the materials used in the HCB to arrive at more specific load and resistance factors. For now, due to the similarities of the HCB to a reinforced concrete beam, it seems reasonable to use the load and resistance factors in the AASHTO and AREMA codes to safely design an HCB Bridge. The factored demand required by these codes for shear, bending, fatigue and deflection limit states have all been consistently substantiated through laboratory testing of prototype beams.

2.2 DEFLECTIONS

Deflection of a structure is a serviceability limit state that usually has to be satisfied, regardless of the intended use of the structure. It is important to address this limit state first, as FRP structures are very sensitive to meeting the deflection requirements of most structural codes. In fact, designing for deflection criteria has consistently been one of the major constraints to the wide spread use of FRP structures in civil applications, and was the primary factor influencing the conception of the HCB.

The major difficulty in satisfying the deflection limit state with FRP structures is that although these materials have excellent strength characteristics, they still have a relatively low elastic modulus, resulting in less rigidity in the structural members and subsequently larger deflections. As a result, the design of these structures for civil applications generally requires an excessive amount of material over what is required to meet the strength limit states. Subsequently, all economy is lost. The embodiment of the HCB uses lesser expensive concrete and steel to meet the deflection limit state. Based on bridges built to date, serviceability still governs design of the HCB, but the over-design for strength is substantially reduced over that of a homogenous FRP beam, resulting in a more economical structure. In fact, it would be possible to force the bending strength limit state to control design simply by using lower grade steel for the tension reinforcing. However, currently there is no compelling reason to switch to lower strength steel.

It is important to note that in most conventional concrete bridge structures the cross-sections of the girders are prismatic, i.e. constant over the length of the beam. For simply supported beams, this grossly simplifies deflection calculations. Where cross-sectional properties vary over the length, the assumption of a constant flexural rigidity (EI) over the length is no longer valid. Variation in the rigidity over the length of the beam has to be taken into account, even for simply supported beams. Such is the case with the HCB.

In order to account for the variable location of the compression strut along the length of the beam, the section properties for the HCB are generally calculated at 1/10th points along the length. The Moment Area Theorem is used to calculate the deflection of the beam at mid-span performing a numerical integration of the controlling live load moment diagram and the variable section properties. This results in very accurate calculation for simply supported structures. For continuous structures it is still easier to calculate the live load deflections using a matrix analysis or finite element program.

The deflected shape of a simply supported beam is depicted in Figure 2.2. The slope of the tangent to the deflected shape from the left end of the beam can be calculated as follows:

$$\theta = \int \frac{M(x)dx}{EI}$$

2.3 POSITIVE MOMENT BENDING

Bending failure is undoubtedly one of the more critical strength limit states. For the HCB, the ultimate bending limit state is analogous to a reinforced concrete beam in many ways. In evaluating the ultimate strength design of reinforced concrete it is assumed that the concrete below the neutral axis has cracked, is in tension and no longer contributes to the strength of the beam. Plane sections are assumed to remain plane, but the stresses in the concrete are not linearly proportional to strain at ultimate. Although the HCB contains materials that are generally new to most practicing structural engineers, with a basic understanding of the mechanics of Bernoulli-Euler beam theory and a working knowledge of standard bridge design codes, it is not difficult to assess the load carrying capacity of the HCB. In fact most design codes, including AASHTO and AREMA are compartmentalized and allow the engineer a fair amount of flexibility in assessing how forces are resisted by a structure. Further, the applied loads as well as the load and resistance factors can easily be rationalized for assessing the response and structural capacity of the HCB.

For simplification in calculations, it is assumed that at the ultimate strain, the concrete stress remains constant over the entire depth in compression. The magnitude of this constant stress is assumed to be some portion of the ultimate compressive stress in the concrete. The most commonly used value in the United States is the limiting value of $0.85f_c'$, where f_c' is the strength of the concrete determined from test cylinders. This equivalent stress is then applied over a depth, "a" which is some portion of the total depth of concrete above the neutral axis. This limiting stress applied over the specified depth results in a compression force that is equivalent to what would be found from a rigorous integration of the actual stresses in the concrete loaded in compression. Although there are several models that have been derived for this purpose, the one described above is commonly known as "Whitney's Equivalent Stress Block", and can be found in most reinforced concrete textbooks.

By assuming the compressive stress in the concrete at failure, it is possible to ascertain the amount of tension reinforcing required for a concrete beam by equilibrating the tension force with the compression force in the concrete. A balanced design and subsequently a ductile failure mode are assured in reinforced concrete beams by limiting the amount of the reinforcing steel such that the steel will yield prior to crushing of the concrete. When the failure mode becomes crushing of the concrete, the beam is considered to be over reinforced.

As mentioned before, the amount of tension reinforcing required for the HCB is typically governed by satisfying the deflection criteria. As a result, whether steel, glass or carbon is utilized for the tension reinforcing, in most cases all of the materials except the compression reinforcement will remain in the elastic region. As a result, at ultimate bending capacity, the failure mode for the hybrid-composite beam is likely to be crushing of the compression reinforcement rather than a ductile failure of the tension reinforcement or failure of the laminate. Noting these differences, it is now possible to describe the methodology in calculating the ultimate bending capacity of the HCB.

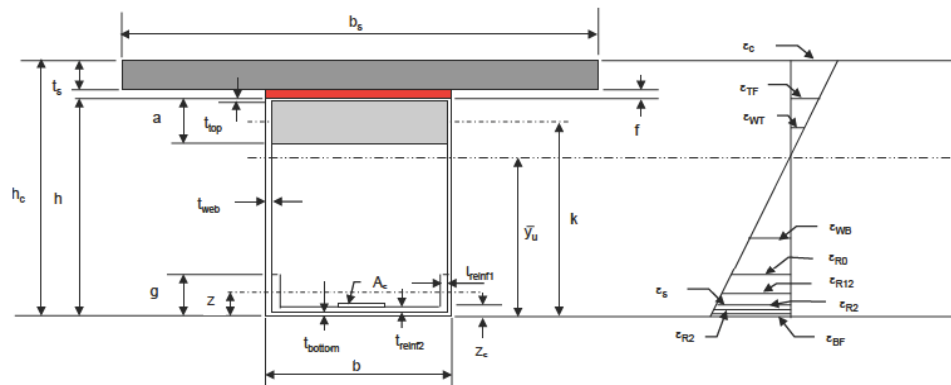


Figure 2.3 Typical HCB Cross-Section & Strain Diagram

Bridge B0439

HCB-Maintenance Manual

August 2012

The typical cross-section for an HCB along with the strain components of the various elements of the beam can be generically defined by the drawing in Figure 2.3. Based on these assumptions it is possible to ascertain the strain in each component of the beam using strain compatibility. The various components of the HCB are defined by the following dimensional variables:

Dimensional Variables

Variables	Dimension	Description
h_c	Inches	Total depth of composite section (deck and fillets inclusive)
b_{eff}	Inches	Effective slab width of composite concrete deck
h	Inches	Depth of HCB
a	Inches	Depth of compression reinforcement, a.k.a. Arch (trial value approximately $h/8$)
b	Inches	Width of HCB shell
b'	Inches	Width of compression reinforcement (Arch)
z	Inches	Distance to centroid of side reinforcement relative to bottom of beam (optional)
g	Inches	Height of side reinforcement (optional)
k	Inches	Distance from bottom of beam to centroid of compression reinforcement
t_{top}	Inches	Thickness of FRP shell top flange (input in layers)
t_{bottom}	Inches	Thickness of FRP shell bottom flange (input in layers)
t_{rein2}	Inches	Thickness of supplemental tension reinforcing along bottom flange (input in layers)
t_{rein1}	Inches	Thickness of supplemental tension reinforcing side return (input in layers)
t_{web}	Inches	Thickness of FRP shell webs (input in layers)
A_s	in^2	Area of steel reinforcement (typically prestressing strand)
z_s	Inches	Distance to centroid of steel reinforcement relative to the bottom of beam
t_s	Inches	Thickness of composite concrete deck
f	Inches	Minimum fillet height (fillets neglected in section property calculations)

The strain in each individual component can be derived using similar triangles based on a prescribed value for the strain in the top fiber of the concrete, " ϵ_c ". The equation for each component of an HCB acting compositely with a concrete deck is shown below.

The strain in the Top Flange of HCB shell:

$$\epsilon_{TF} = \epsilon_c \frac{h - \bar{y}_u}{h_c - \bar{y}_u}$$

The strain in the top portion of the HCB shell webs in compression:

$$\epsilon_{WT} = \epsilon_c \frac{h - \bar{y}_u}{2(h_c - \bar{y}_u)}$$

The strain in the bottom portion of the HCB shell webs in tension:

$$\epsilon_{WB} = \epsilon_c \frac{-\bar{y}_u}{2(h_c - \bar{y}_u)}$$

The strain in the bottom flange of the HCB shell:

$$\epsilon_{BF} = \epsilon_c \frac{-\bar{y}_u}{(h_c - \bar{y}_u)}$$

The strain in the fabric tension reinforcing (typically steel or carbon) along bottom of the HCB shell:

$$\epsilon_{R2} = \epsilon_c \frac{t_{bottom} + t_{rein2} / 2 - \bar{y}_u}{(h_c - \bar{y}_u)}$$

The strain in the side return portion of fabric tension reinforcing (typically steel or carbon) of the HCB shell:

$$\epsilon_{R11} = \epsilon_c \frac{g - \bar{y}_u}{(h_c - \bar{y}_u)}$$

Bridge B0439

HCB-Maintenance Manual

August 2012

The strain in the triangular portion of the fabric tension reinforcing side return:

$$\epsilon_{R12} = \epsilon_c \frac{\frac{1}{2}(g - t_{bottom-reinf2}) - \bar{y}_u}{(h_c - \bar{y}_u)}$$

The strain in the steel tension reinforcing:

$$\epsilon_s = \epsilon_c \frac{z_s - \bar{y}_u}{(h_c - \bar{y}_u)}$$

The stress in each component of the HCB can then be calculated by multiplying the strain values by the respective moduli of elasticity values for each material using the following equation for Hooke's Law, where "i" signifies the component under consideration:

$$\sigma_i = E_i \epsilon_i$$

The force in each component of the beam can then be calculated by multiplying the stress times the respective area for each component using the equations below starting with the deck slab. The compression force in the composite concrete deck is calculated assuming that the compressive strain in the concrete ϵ_c has reached an ultimate compressive strain $\epsilon_c = \epsilon_{cu} = 0.003$ using the following equation:

$$F_{cs} = 0.85 f'_{cs} \beta_1 t_s b_{eff}$$

Where f'_{cs} is the ultimate compressive stress of the deck concrete. This equation holds true where the plastic neutral axis is located below the deck slab. However it is possible for the location of the neutral axis to be located within the deck slab itself, in which case the force in the deck becomes:

$$F_{cs} = 0.85 f'_{cs} \beta_1 x b_{eff}$$

Where β_1 is 0.85 for $f'_{cs} = 4,000$ psi concrete and a variable $x = h_c - \bar{y}_u$. The value of $\beta_1 x$ defines Whitney's equivalent stress block as is common in reinforced concrete design. The value of β_1 is a function of the ultimate concrete strength.

The compression force in the arch concrete also depends on the location of the plastic neutral axis or PNA. In the case where the PNA falls below the concrete arch concrete, the force in the arch is calculated as follows:

$$F_{CB} = 0.85 f'_{CB} \beta_1 a b'$$

Where f'_{CB} is the ultimate compressive stress in the arch concrete. In the case where the PNA is located within the concrete deck slab, it is assumed that the arch goes into tension and subsequently the force in the arch is set to zero. The other condition is where the PNA is located within the arch, in which case the force in the arch concrete is limited to the concrete above the PNA that is in compression and is thus calculated as:

$$F_{CB} = 0.85 f'_{CB} (\beta_1 x - t_s) b'$$

The other components of the HCB are calculated as a function of the strain in the concrete. The compression force in the FRP top flange of the HCB shell is calculated as follows:

$$F_{TF} = E_{TF} \epsilon_c \frac{h - \bar{y}_u}{h_c - \bar{y}_u} b t_{top}$$

The compression force in the portion of HCB shell webs located above the plastic neutral axis:

$$F_{WT} = E_w \epsilon_c \frac{h - \bar{y}_u}{2(h_c - \bar{y}_u)} t_{web} (h_c - \bar{y}_u)$$

The tension force in the portion of HCB shell webs located below the plastic neutral axis:

Bridge B0439

HCB-Maintenance Manual

August 2012

$$F_{WB} = E_w \epsilon_c \frac{-\bar{y}_u}{2(h_c - \bar{y}_u)} t_{WB}(\bar{y}_u)$$

The tension force in the FRP bottom flange of the HCB shell:

$$F_{BF} = E_{BF} \epsilon_c \frac{-\bar{y}_u}{(h_c - \bar{y}_u)} b t_{bottom}$$

In some cases, supplemental tension reinforcing can be added that has both a bottom flange and a side return component. This type of reinforcing could be carbon or steel fibers of some other type of fabric reinforcing. In many cases, this element of tension reinforcing is omitted in which case the respective force contributions are zero. For simplicity of calculation, the force in the side returns is quantified as a constant stress (rectangular) portion of the stress trapezoid. The other portion is a triangular stress distribution. The force in the bottom flange portion of this supplemental tension reinforcing is calculated as follows:

$$F_{R2} = E_{R2} \epsilon_c \frac{t_{bottom} + t_{rein2}/2 - \bar{y}_u}{(h_c - \bar{y}_u)} b t_{rein2}$$

The tension force in the portion of the supplemental reinforcing with a constant (rectangular) stress component is as follows:

$$F_{R11} = E_{R2} \epsilon_c \frac{g - \bar{y}_u}{(h_c - \bar{y}_u)} 2 t_{rein1} (g - t_{bottom} - t_{rein2})$$

The tension force in the portion of the supplemental reinforcing with a triangular stress component is:

$$F_{R12} = E_{R2} \epsilon_c \frac{(g - \bar{y}_u) - [\frac{1}{2}(g - t_{BOT} - t_{rein2}) - \bar{y}_u]}{(h_c - \bar{y}_u)} [2(t_{rein1})(g - t_{bottom} - t_{rein2})]$$

In some cases, the supplemental tension reinforcing can be steel fabric. In this case, if the strain in the steel exceeds the yield strength of the material, the force is limited to a stress calculated based on the yield strength of the steel used. If this supplemental tension reinforcing is FRP and the limiting strain is exceeded, the forces in these components are set to zero as the FRP materials are generally linear elastic to failure and then carry no additional load after rupture.

The last component of the beam is the tension reinforcing, which is typically steel. The force in this component is calculated as follows:

$$F_s = E_s \epsilon_c \frac{z_s - \bar{y}_u}{(h_c - \bar{y}_u)} A_s$$

Again, if the strain in the steel tension reinforcing exceeds the yield strain of this material, then the force in the steel is calculated using a limiting stress equal to the yield strength of the steel. Hence the force in the steel becomes:

$$F_s = f_y A_s$$

Where f_y is the yield strength of the steel being used.

Once all of the horizontal force components in the HCB are known, the exact location of the plastic neutral axis can be found directly from force equilibrium on the section with the simple equation:

$$\Sigma F = F_{CS} + F_{CB} + F_{TF} + F_{WT} + F_{WB} + F_{BF} + F_{R2} + F_{R11} + F_{R12} + F_s = 0$$

By definition, the HCB has several different materials each with different constitutive properties. To simplify the calculations, it is easiest if all the materials are normalized to the constitutive properties of one material. Historically, the

Bridge B0439

HCB-Maintenance Manual

August 2012

best solution has been to normalize all the materials to the properties of the glass FRP laminate in the HCB shell. This is the philosophy typically followed for the deflection calculations as well, where all of the section properties are calculated based on dimensions normalized by the ratios of Young's modulus of elasticity for a given material to that of the FRP laminate as follows:

$$n_c = \frac{E_{concrete}}{E_w} = \text{Modular ratio of concrete to FRP webs}$$

$$n_R = \frac{E_{reinforcing}}{E_w} = \text{Modular ratio of supplemental tension reinforcing to FRP webs}$$

$$n_s = \frac{E_{steel}}{E_w} = \text{Modular ratio of steel tension reinforcing to FRP webs}$$

In general it is usually assumed that the laminate in the FRP shell is relatively constant, in which case:

$$E_{TF} = E_{BF} = E_w$$

Subsequently, all calculations are made using the modulus of elasticity of the FRP webs. It should be noted however that although this is an acceptable assumption to calculate strains, the proper modular ratios must still be used in calculating the actual stress in each given material.

Knowing all of the force equations for each component and normalizing each component to the properties of the FRP shell, it is now possible to return to the force equilibrium equation and solve directly for the plastic neutral axis using the following equation:

$$\bar{y}_u = \frac{[bt_{top}h + t_{web}h^2 + \frac{0.85h_c(f'_{CS}t_s b_{eff} + f'_{CB}ab)}{E_w \epsilon_c} + 3n_R t_{Reinf1} g^2 + n_s z_s A_s]}{[bt_{top} + 2t_{web}h + \frac{0.85(f'_{CS}t_s b_{eff} + f'_{CB}ab)}{E_w \epsilon_c}] + bt_{bottom} + n_R b t_{Reinf2} + 2n_R t_{Reinf1} g + n_s A_s}$$

The closed form solution offered above is based on the assumption that the PNA is below the arch concrete. As noted previously, if the PNA is within the arch concrete or within the deck slab, the force components for these elements need to be revised accordingly. The subsequent derivations are left to the reader. For simplicity, the same calculation is performed in a spreadsheet calculation. In the programmed version, the user assumes a location for the PNA, the program then calculates the corresponding strains and forces. If the sum of the horizontal forces within the section is not in equilibrium, the program assumes a new location for the PNA. This calculation sequence is repeated until the program converges on and PNA location that results in internal equilibrium.

Once the exact location of the PNA has been established, the nominal moment resistance capacity can be calculated by summing the moments around any point in the cross-section. For simplicity, the PNA can be used as the point to sum moments about. Subsequently, the equations for the respective moment arms for each component of the HCB about the PNA can be defined as follows:

$$d_{CS} = -(h_c - \bar{y}_u - \frac{t_s}{2})$$

$$d_{CB} = -(h - \bar{y}_u - t_{top} - \frac{a}{2})$$

$$d_{TF} = \bar{y}_u - (h - \frac{t_{top}}{2})$$

$$d_{WT} = -\frac{2}{3}(h - \bar{y}_u)$$

$$d_{WB} = \frac{2}{3}(\bar{y}_u)$$

Bridge B0439

HCB-Maintenance Manual

August 2012

$$d_{BF} = \bar{y}_u - \frac{t_{bottom}}{2}$$

$$d_{R2} = \bar{y}_u - t_{bottom} - \frac{t_{R2}}{2}$$

$$d_{R11} = \bar{y}_u - \frac{1}{2}(g + t_{bottom} + t_{R2})$$

$$d_{R12} = \bar{y}_u - \frac{g}{3} - \frac{2}{3}(t_{bottom} + t_{R2})$$

$$d_s = \bar{y}_u - z_s$$

In addition to the typical resistance factor of 0.9, the resistance is also multiplied by an additional 0.9Φ factor as suggested in ACI 440 to compensate for knock down factors on FRP laminates. The calculated nominal moment capacity is compared to the factored demand to validate that the section has adequate capacity. The equations are valid for any section and typically the capacity is checked at $1/10^{\text{th}}$ points for the HCB without the concrete slab. For the maximum moment with the composite concrete deck, the section is typically only checked at mid-span. This is based on the fact that once the deck is cast on top of the beam, assuming the amount of steel remains constant along the length of the beam, then the bending capacity at other points along the beam is essentially constant.

The rigorous calculation detailed above provides an accurate and rational method of calculating the bending strength capacity of the HCB consistent with generally accepted structural design codes and specifications. Alternatively, one can generally get an approximate answer within 5% to 10% of the exact answer, simply by taking the compression force in the concrete, i.e. the slab and/or arch, and equilibrating it to a tension force in the steel, or in other words, the nominal moment capacity of the section is as shown in the following question:

$$\phi M_n = C(d - a/2)$$

$$\Phi M_n = C(d - a/2)$$

Where: Φ = resistance factor for bending

M_n = nominal moment capacity

$C = f_c' ab$ (the compression force in Whitney's equivalent stress block)

d = the distance from the centerline of the steel reinforcement to the top of the beam

a = the depth of concrete in compression

Although in the case of a compression strain failure of the concrete, the HCB no longer conforms to the elusive, slow ductile failure mode, it should be noted that there are not very many documented cases of this failure mode resulting in a collapse in real life structures. For cases where it is deemed necessary or desirable, there are ways to create this ductile, tensile failure in the HCB. For example, by using a lower grade steel, supplementing lower grade steel for deflections only or when possible simply by building multi-span bridges where the HCB is made continuous for live load by providing negative moment reinforcing steel over the supports as has been done on several structures to date.

2.4 NEGATIVE MOMENT BENDING

Although originally conceived as a simply supported member, the HCB can also be made continuous for live loads. This is done by placing negative moment reinforcing steel in the deck over the piers and diaphragms. The calculation of the resistance is conducted in much the same manner as for positive bending, but with the strain diagram reversed to reflect tension stresses in the top of the section and compressive stresses in the bottom of the section.

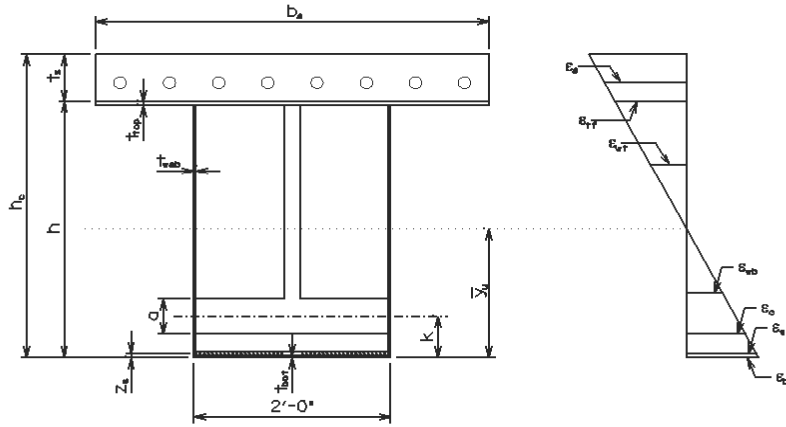


Figure 2.4 – Strain Distributions for Negative Bending

For sections directly over the piers, the strain components in the FRP shell and strands can be completely discounted and the negative bending capacity is no different than for a conventional reinforced concrete beam where the arch is the compression block and the rebar in the deck is the tension reinforcing. For sections away from the supports, the resistance can be checked assuming some contribution from the FRP shell. In most cases, the HCB has sufficient capacity that even if a plastic hinge is formed over the intermediate piers, the HCB still has adequate capacity to carry the specified loads as a simply supported beam.

Bridge B0439

HCB-Maintenance Manual

August 2012

2.5 VERTICAL SHEAR

Similar to concrete and steel, shear behavior of the HCB is a bit more complex than bending. In the HCB, shear resistance is facilitated by three mechanisms acting in concert. To start with, the primary reason for the arch shape of the compression reinforcing in the HCB is to carry a significant portion of the shear as direct compression forces down to the thrust line and into the bearings. Another significant component of the shear mechanism is that the quad-weave fabrics in the HCB shell provide tremendous shear capacity due to the ± 45 degree plies in the laminate. Finally, the third mechanism involves a thin concrete web (typically on the order of 3 inches) that extends vertically along the longitudinal centerline of the beam between the top of the arch and the bottom of the supported deck. This concrete web is actually monolithic with the arch concrete when cast. Further, the diagonal shear connectors extending from the arch to the deck provide for very efficient reinforcing of this concrete web.

The composite action between the HCB and the supported deck is facilitated through the shear connection device that is comprised of galvanized reinforcing bars spaced at typical intervals of roughly 12 inches. These bars are placed at 45-degree angles and have a 90-degree hook at both ends. One of the hooks is connected under a continuous $\frac{1}{2}$ inch diameter steel strand lying in the bottom of the arch rib. The other hook is developed into the concrete deck. These shear connectors are basically designed like inclined stirrups in a reinforced concrete beam, with the number of connectors being sufficient to develop the full factored moment acting on the section in bending. The fragmentary perspective in Figure 2.5 provides a schematic detailing all of the main components of a typical HCB.

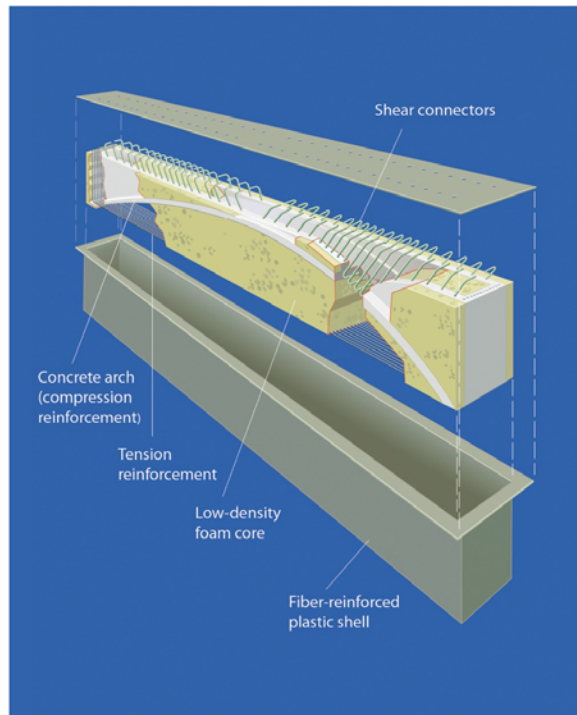


Figure 2.5 - Fragmentary Perspective of a typical HCB

In quantifying the shear resistance of the HCB, the first component to consider is the thrust in the arch at a given section. The thrust can then be discretized into horizontal and vertical components. The vertical component can be deducted from the gross shear on the section as the arch is resisting this. The remaining shear is then resisted primarily by the FRP webs, but also by the thin concrete web above the arch. This results in a hybrid resistance to the shear forces in the beam, but there are some other interesting facets of the shear behaviour that very much emulate a reinforced or prestressed concrete beam. For example when the loads are applied to the structure to produce maximum shear effects, e.g. adjacent

Bridge B0439

HCB-Maintenance Manual

August 2012

to a support, the majority of the shear is resisted strictly through the arching action similar to the strut and tie behavior (Collins, et al. 2008).

Further, because the principal stresses in the beam are oriented along the arch and there is no concrete within the tensile zone of the beam to crack, in essence the concrete cannot crack and as a result it is not necessary to rely on Modified Compression Field Theory (MCFT). Instead of relying on steel reinforcing in the concrete, the horizontal shear between the arch and the tension reinforcing is carried by the FRP laminate and since the laminate is bonded to the foam core along a continuum, it is possible to develop the full capacity of the FRP laminate up to the factored shear demand. This behaviour has been validated in numerous laboratory tests on prototype beams for each installation of the HCB done to date.

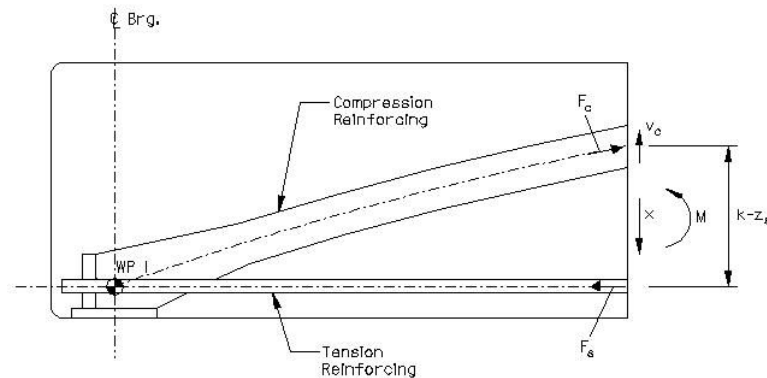


Figure 2.6 - Free Body Force Diagram Showing Shear Component in Compression Reinforcing

The free body diagram shown in Figure 2.6 demonstrates evaluating the reduction in the shear force in the webs of the HCB. This figure shows the internal forces acting on the compression and tension reinforcing. The component of shear taken by the compression reinforcing is V_c . The magnitude of V_c is calculated by dividing the moment at this section by the moment arm ($k-z_b$) to get the axial force in the tension reinforcing, which is equal to the horizontal component of the force in the compression reinforcing. Knowing the slope of the compression reinforcing at the given location, it is then possible to calculate the vertical component, V_c , of the resultant compression force. As the profile of the compression reinforcing is a continuous parabolic arch, it is easy to calculate the slope of the compression reinforcing at any given point by simply taking the first derivative of the continuous function for the profile of the arch. The equation for calculating the net shear on a section then becomes:

$$V_{net} = V - M \frac{k'}{(k - z_g)}$$

In this equation (k') is the slope of the profile at the given location. It is important to note that due to the nature of moving loads, an accurate calculation for the net shear requires that the moment used in this equation be calculated for the same position of the live load that is used for calculating the shear, i.e. corresponding moments and shears. It is also important to note that the reduction in web shear force due to arching action is also predicated on the assumption that there is no shear or bending in the compression reinforcing, i.e. it is in pure compression and the resultant compression force is coincident with the profile of the arch.

2.6 HORIZONTAL SHEAR

In most cases it is desirable to engage composite action between the deck slab and the HCB for the significant increase in bending stiffness and subsequent reduction in live load deflections. Depending on the specific project, composite action between the deck and HCB may also be required for bending strength. Regardless, some rational basis for the design limit state of this reinforcing is required. The methodology created for the shear transfer between the beam and the

overlay also provides for a positive method of connection between the beam and overlay. This device is even more important in bridge applications where the beams are made composite with the supported concrete deck for strength purposes as well as satisfying deflections.

The shear connectors used to connect the deck to the HCB are typically galvanized reinforcing bars placed on a 45 degree incline with one end embedded in the concrete of the compression arch and the other end embedded in the concrete slab. A schematic view of a series of shear connectors in an HCB can be seen in the cut-away elevation of half a beam as shown in Figure 2.7. The embedding of the shear connectors in the arch and slab results in a very efficient use of the shear connector as a tension member. The compression forces in the slab are transmitted into the shear connector and transferred directly into the compression arch where they are carried to the bearings as depicted in the strut and tie model shown in Figure 2.8. This load path does not require any of the compression force in the slab to be transmitted as shear forces in the FRP webs.

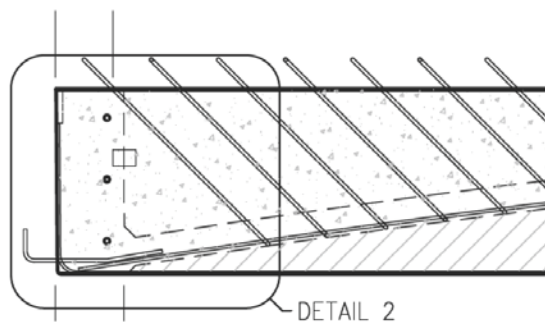


Figure 2.7 - Cut-Away of Beam Elevation with Shear Connectors

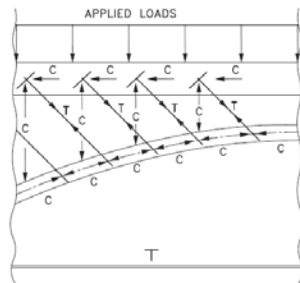


Figure 2.8 - Strut-and-Tie Model of Shear Stud Behavior

Although the shear connector for the HCB serves the same purpose as the shear connectors in conventional beams, the fact that it is positioned on a 45 degree angle results in a slightly different behavior. Regardless, the shear-friction design method contained in Article 11.7.4 of ACI-318 provides a rational method of quantifying the shear strength of this type of connection device. Using equation (11-27) from this section we get:

$$V_n = A_{vf} f_y (\mu \sin \alpha_f + \cos \alpha_f)$$

- Where: V_n = nominal shear capacity of one connector
- A_{vf} = shear area of one connector
- f_y = yield strength of shear connector
- μ = coefficient of friction between top of HCB flange and concrete overlay (anticipated to be similar to concrete anchored to as-rolled structural steel, or 0.7 for normal weight concrete)

Bridge B0439

HCB-Maintenance Manual

August 2012

α_f = angle between shear-friction reinforcement and shear plane

Whereas this equation quantifies the shear capacity of a single connector, the number of connectors required for ultimate strength would be determined in accordance with the provisions of Article 10.38.5.1.2 in the AASHTO Standard Specification for Highway Bridges. In this provision it is assumed that the number of shear connectors provided must be sufficient to develop the total ultimate compression force in the supported concrete slab. It also assumes that all of the connectors will have reached their ultimate capacity in order to develop the compression force in the slab.

It should be noted that two other criteria need to be evaluated in order to quantify the shear capacity of the connectors including: the compression failure cone of the concrete located around the anchorage of the stud as well as the fatigue capacity of the stud assembly under the requisite number of live load cycles. In most cases, the shear connectors used for the HCB comprise conventional rebar with a 90-degree hook at both ends for development. The hook on the lower end is developed around a piece of strand draped along the bottom of the arch concrete. The hook on the top end is tied into the deck steel for the structural concrete slab. Subsequently, the shear connectors behave more like conventional, horizontal shear reinforcing steel than shear studs on a steel beam. Laboratory testing done to date appears to indicate that the shear connectors are adequately designed and developed to resist the anticipated forces and that fatigue loading does not compromise the capacity.

2.7 FATIGUE CONSIDERATIONS

To date, extensive fatigue testing has been performed on at least five laboratory specimens as well as a complete railroad bridge subjected to real Class 1 freight rail traffic. These specimens have been subjected to anywhere between 500,000 to 2,000,000 cycles of fatigue without any change in performance. In particular, the first 30-foot railroad bridge tested in Pueblo, CO was subjected to 237 Million Gross Tons (MGT) of heavy axle Class 1 traffic (this equates to roughly 1,500,000 cycles of service load Cooper E-80 loading).

In evaluating the behavior of the HCB for fatigue, consideration should be given both to materials as well as the interface between the major components of the beam. Regarding the compression reinforcing, the concrete in the HCB is essentially in compression at all times. Concrete in compression is not subject to fatigue failures. The FRP laminates and the steel tension reinforcing are subjected to tensile stresses. However, in most applications to date, the live load, tensile stress ranges in these materials are on the order of 10% of the ultimate capacities. Subsequently, there currently appears to be no cause for concern regarding fatigue in the FRP or the steel tension reinforcing.

One exception to this matter is when the design allows for omitting steel for the tension reinforcing and just using additional glass fabric for the tension capacity. This has been done successfully on a couple of different occasions. However, when this is the case, the limiting sustained stress levels in the laminate due to sustained dead loads should be limited to within 25% of the ultimate capacity to prevent creep rupture.

Lastly, there is the overall system consideration of what happens between the interfaces for the various materials. Again, all fatigue cycling conducted to date tends to dismiss any concern for hysteresis that could result in an overall change in the stiffness of the system due to breaking down the interfaces between the different materials.

2.8 LOAD RATING METHODOLOGY

Load Rating for an HCB highway bridge can be performed using the standard methodology and equations published in the AASTHO Load and Resistance Factor Rating Specifications (LRFR) for both inventory and operating conditions. These ratings are typically done for the ultimate bending limit state. As discussed previously, the shear limit state still requires further evaluation to develop an accurate mathematical model for predicting the failure limit state for shear. In the interim, load tests in the laboratory have consistently indicated shear capacities well beyond two times the code specified factored demand.

3.0 MATERIAL & STRUCTURAL DAMAGE SERVICEABILITY CONSIDERATIONS

This section of the manual is intended to provide information relative to some types of material and structural damage that could result from environmental conditions or other potentially catastrophic events that are not necessarily addressed in the codes. These items include things like UV degradation of the laminates, fire resistance, thermal loads and lateral impact. The information provided is primarily to make the owner aware of conditions that could impact the long-term performance of the HCB and where practicable, provide suggestions for mitigation if one of these issues is encountered during the service life of the HCB Bridge.

3.1 ULTRAVIOLET RADIATION

Solar ultraviolet (UV) radiation exposure is known to be deleterious to organic materials, including polymer resins. There is some evidence that the effect of UV radiation may be limited to cosmetic degradation of the resin in the surface of the laminate and that there is no impact to the structural properties of the FRP laminate. In some ways this is no different from a thin layer of patina that might form on weathering steel.

Visual evidence of degradation from UV radiation can be observed by change in the surface color, loss of pigment and/or loss of luster to the surface of the laminate. Although the degradation is generally confined to a thin layer on the surface, studies have been conducted to quantify the degradation of bulk tensile properties in a vinyl ester matrix (Signor, Chin). The degradation on the resin usually manifests itself as a decrease in the ultimate strain and a decrease in the specific toughness of the surface layer of the resin. This results in an increase in the surface modulus of elasticity combined with a greater propensity for the propagation of cracks in the surface. Consequently, given the inevitable exposure of a bridge girder to UV radiation, it would be undesirable to leave the surface layer of the laminate exposed to sunlight.

Additives have been included in the resin formulations to help stabilize the resins against UV degradation. Another common method to mitigate UV concerns that also enhances the aesthetic appearance is the application of a gel coat. A gel coat is a thick resin layer on the exterior surface of the laminate that can be sprayed into the mold prior to lay-up and infusion of the laminate. The gel coat can also be spray or roller applied subsequent to the manufacturing of the composite. The gel coat is typically a different type of resin than that used for the matrix of the FRP laminate, but the gel coat resins are usually formulated to be compatible with specific resins. In addition to the UV protection and improved surface finish, the gel coat also serves as an excellent surface barrier against moisture intrusion and enhances the fire resistant and/or flame spread qualities of the FRP laminate.

The standard practice with HCB bridges fabricated to date is to utilize UV inhibiting admixtures in the pigments mixed in with the resin. In addition, a post-applied gel coat paint is generally rolled onto any fascia beams or other surfaces that are anticipated to receive direct sunlight. Unlike steel, the substrate under the gel coat will not rust. Subsequently, it is not anticipated that the gel coat will need to be removed and reapplied on a periodic basis. Regardless, the surface should be checked during biennial inspection to look for any loss of bond, or peeling that might warrant reapplication. Note that failure to repair the gel coat surface constitutes more of a cosmetic issue than any concern for accelerated deterioration of the laminate. The UV inhibiting pigments are still contained in the resin and although the surface may fade and become chalky, the strength of the laminate should not be compromised.

3.2 FIRE RESISTENCE

One question that continually arises regarding composites relates to the susceptibility of fire damage. The threat of fire for bridges generally ranges somewhere between an errant brush fire to a tanker truck exploding on, or underneath a bridge. Given the range of possible fire events, bridge codes have never really committed to quantifying an event that has to be satisfied in design. Regardless, this is a concern for a bridge owner and subsequently this issue has been investigated to determine measures that could help mitigate the severity of these events. Although not addressed in bridge codes, fire resistance does become a significant issue in building structures or other occupied spaces.

When required, quantification of fire test response is usually determined through ASTM E84-05 "*Standard Test Method for Surface Burning Characteristics of Building Materials*". The HCB's fabricated to date have all been infused using a Bisphenol-A, Epoxy Vinyl Ester resin that is generally combined with styrene to lower the viscosity for infusion. In a nutshell, these resins will burn with a sustained ignition source applied. Whereas it is almost impossible to fabricate a bridge structure that can resist any fire event, the resins can be formulated with Bromine or Aluminum Tetra hydrate to at least develop self-extinguishing characteristics that will reduce the likelihood of burning unless a continuous ignition source is applied. Although these additives will help facilitate self-extinguishing properties for the laminate, they can make the infusion process more difficult due to changes in the viscosity of the resin.

Bridge B0439

HCB-Maintenance Manual

August 2012

Another test related to fire resistance is ASTM E119 “*Standard Test Method for Fire Tests of Building Construction and Materials*”. The purpose of this test is to look at the ability of a structural system to contain a fire or to retain its structural integrity, or both, during the test and to measure the endurance of the system in time. Again although this test has been used to quantify the performance of building structural systems since 1918, there are no prescribed endurance limits for bridge structures.

In any case, it should be noted that 90% of the strength and stiffness of the HCB still comes from concrete and steel. Even with an applied heat source, the bridge will likely be able to sustain loads under fire for at least as long as a similarly designed steel girder bridge. It should also be noted that the polyisocyanurate used for the foam core has tremendous R-values on the order of 5.4 hour-sf²-°F/BTU. In fact the most common application of this product is for thermal insulation. For fires that are confined to the top of a bridge, the HCB’s will also be insulated from the fire by the concrete overlay or deck placed on top of the beams.

3.3 THERMAL EXPANSION

Differential movement due to thermal expansion and contraction is prevalent in all types of structures. The combination of materials in the HCB warrants discussion regarding this topic. In general, the coefficient of thermal expansion (CTE) of an FRP component is highly dependent on the type of resin as well as the type and orientation of the reinforcing fabrics. In pultruded shapes, where most of the reinforcing is in the longitudinal direction, the CTE in the transverse direction can be an order of magnitude different from the CTE in the longitudinal direction. The laminates in the HCB typically use a quad-weave fabric with fibers running in four different directions. As a result, the CTE tends to be very consistent between the transverse and longitudinal directions. Further, ASTM D696 tests were conducted on 14 samples of witness panels fabricated as part of the QC/QA process for the Knickerbocker Bridge to determine the CTE. The average value was found to be approximately 7.0×10^{-6} /deg F. This is almost identical to the CTE’s for concrete and steel. As a result, thermal strains induced in the HCB will not result in any shear between the interfaces of the different materials used. This has also been validated through testing at the University of Maine.

3.4 LATERAL IMPACT

Another issue that comes up quite frequently has to do with the resulting damage that might occur in the event that an HCB bridge is impacted transversely from an over-height vehicle passing under the bridge. Like the issue of fire resistance, this is an issue that is not directly addressed in the AASHTO design codes, but is a legitimate concern. In one study back in 1980, it was documented that about 120 prestressed concrete girder bridges are damaged in the United States each year by impact from over height vehicles (Shanafelt and Horn). Figure 3.1 demonstrates an extreme example of this type of impact. In all likelihood, there are probably even more girders damaged that are not reported. Further, it is likely that an equal or greater number of steel bridges are also impacted each year. Given this frequency of impact, the probability of an HCB bridge being impacted by an over-sized vehicle almost becomes inevitable once a significant number of these bridges have been deployed. The questions that arise are; what kind of damage will be sustained by the HCB for similar impact loads, will an impact load result in collapse of the bridge and how will the HCB damage from an impact be repaired.



Figure 3.1 Photos Showing Prestressed Beam Bridge Impacted by Over-Height Vehicle

Bridge B0439

HCB-Maintenance Manual

August 2012

The first two questions are not easily answered without experimental data. Vessel and or vehicle collision impact loads applied to bridge substructures are well documented, however there is no specific design load quantified for impact of a bridge girder by an over-height vehicle. In a study conducted at Iowa State University, Abendroth and Fanous performed analytical evaluations of impact loads applied to prestressed concrete girder bridges. As part of this study, impact durations for vehicle crashes were evaluated to arrive at a reasonable load for the analysis. The loads contrived comprised a constant-magnitude force of 120 kips for loads applied directly at a diaphragm location and 60 kips if applied at a location along the bottom of the beam away from a diaphragm. The primary objective of the Iowa State study was to compare the behavior of the bridge under impact loads with steel diaphragms versus concrete diaphragms.

The intent is not to make comparisons between the Iowa State study and the behavior of an HCB bridge, but rather to demonstrate that there is no codified horizontal impact force that must be satisfied prior to deployment of an HCB bridge. That being said, this issue undoubtedly warrants investigation. In general, it is anticipated that the HCB will fair very well under over-height vehicle impact loads due to the highly resilient nature of the FRP laminate. Although the exact nature of the damage from a lateral impact load can only be speculated, Section 5.3 of this report will address how an HCB might be repaired once damage is sustained from vehicle impact.

5.0 INSPECTION AND MAINTENANCE

One of the more pertinent questions consistently raised relates to the inspection and maintenance of the HCB. It is not possible to thoroughly address this concern within the confines of this manual, a good reference is NCHRP Report 564, *Field Inspection of In-Service FRP Bridge Decks*. Although the FRP decks and bridge elements addressed in this report are more consistent with homogenous FRP structures, many of the NDE techniques discussed and explanations of characteristics of FRP performance are applicable to the HCB.

5.1 INSPECTION METHODS

In terms of maintenance and inspection of highway bridges, federal laws mandate that biennial inspections be performed for all bridges on the National Bridge Inventory (NBI). Different states may have different forms and processes that are incorporated as part of these inspections, however most follow recommendations contained in *The Manual for Condition Evaluation of Bridges* published by the American Association of State Highway and Transportation Officials (AASHTO). Due to the fact that composite bridge components have only recently found their way into the NBI, limited information has been available in the past for purposes of inspecting these types of bridges.

Although composite structures manufactured from pultruded FRP's have been in service for over thirty years, the first all composite vehicular bridges were not really introduced until around 1994. Since that time, nearly one-hundred bridges utilizing FRP composite decks of various types have been constructed in the United States. It was the long-term monitoring and evaluation of these bridges that prompted the National Cooperative Highway Research Program (NCHRP) to commission a study related to this subject. What resulted was *NCHRP Report 564 – Field Inspection of In-Service FRP Bridge Decks* (Telang, et.al., 2006).

This study was focused on composite bridge decks, however the characteristics of, and constituent properties of some of the decks investigated are very similar to those of the HCB. Subsequently, most of the information in the report is equally applicable to the HCB. In addition to inspection and maintenance issues, NCHRP Report 564 serves as an excellent reference providing an overview of composite manufacturing for bridge related products and somewhat of an anthology of composite bridge construction to date.

The NCHRP report also contains useful information regarding suggested forms for summarizing inspection data when evaluating composite bridge decks as well as a bridge condition rating table that categorizes the severity of the condition of the bridge components on a scale from 0 to 9, consistent with condition ratings for conventional bridge components as outlined in the *Recording and Coding Guide for the Structures Inventory and Appraisal of the Nation's Bridges* as published by FHWA.

In order to effectively utilize the information in NCHRP Report 564 it is worth noting particular types of damages and defects for which the HCB may be prone. To this extent, Report 564 is primarily useful only in evaluating the FRP components of the HCB. The other components including the internal arch concrete and the embedded steel reinforcing are not addressed in the Report 564.

FRP Laminates: The potential FRP damage types suggested in NCHRP Report 564 include the following list. Comments specific to the HCB have been interjected to provide some guidance to the inspector.

- *Blistering:* To date this has never been seen on an HCB laminate, but might be more evident on an HCB having a gel coat or intumescent paint application.
- *Voids:* To date voids have not been evident in HCB units. In general, the laminates on the HCB are very thin, providing less opportunity for voids during manufacturing.
- *Discoloration:* With the pigments used in the resin, it is difficult to detect discoloration of the resins in the new HCB. This type of damage will likely be more evident with time, such as chalkiness, yellowing or lightening of the color due to UV exposure. This discoloration itself should not be an indication of a problem requiring

mitigation, but may warrant remediation if cracking of the laminate becomes evident. Cosmetic repairs can be made using marine faring compounds or gel coats to fill the cracks.

- *Cracks:* As with concrete, cracking in an FRP laminate can be qualified in different levels of severity. If the cracks are small and do not seem to propagate or increase in severity, no remediation may be necessary. For cosmetic repairs, marine faring compounds or gel coats may be applied. If the cracks appear to be more analogous to tearing or delamination, see the recommendations below.
- *Delamination:* Delaminations have been evident in laboratory testing of HCBs, but only at loads in excess of factored demand. The types of delamination observed generally relates to the debonding of the web laminate from the interior polyiso core. These types of delamination appear to be as a result of high shear loadings causing tension field action in the webs and have usually been obvious from visual observations. As the webs exhibit elastic buckling in shear, portions of the web can delaminate from the foam. This does not necessarily indicate a compromise in the beam capacity. Regardless, if it is clear that the foam has delaminated from the laminate, restoring the bond between the components is desirable.

Although this process has never been necessary, one recommendation would be to perform a vacuum infusion of adhesives or vinyl ester resins by drilling a select number of holes in the laminate in strategic locations. A vacuum line should be connected at the highest point and resin feed lines attached to the other hole(s). A low viscosity MMA might provide the best solution. *(Under no circumstances should the voids be pressure injected as the pressure from the pump could cause further delamination of the laminate from the foam).*

If the delamination appears to be of greater severity, e.g. if there is a clear separation of laminate layers or sufficient separation to facilitate moisture ingress into the laminate a more substantial repair may be warranted. These types of repairs may require the services of a specialty consultant/contractor. The repairs might include bonding of carbon or glass fibers to reinforce the section to its initial capacity.

- *Presence of Moisture:* FRP laminates are subject to moisture absorption. For the most part, the FRP laminates in the HCB operate at very low strain levels (typically on the order of 10% of ultimate strain). These low strain levels result in less probability of micro cracking in the matrix and reduced absorption rates. If there is evidence of increased propagation of cracking, it may be necessary to evaluate the need for applying a gel coat to the exterior of the HCB as a moisture barrier.
- *Abrasion or tearing:* This type of damage is not anticipated under normal service operations. However this type of damage might occur due to isolated incidents that could result from stream flows at high water levels or from impact from vehicles below the bridge. If there is any concern about loss of section or capacity, repair methods such as those found in ACI 440 should be investigated to strengthen the HCB.
- *Creep, flow, or rupture:* As the stiffness of the concrete and steel components is very high compared to the FRP laminates, the sustained loads and subsequent stresses on the FRP laminates are very low. Subsequently, creep flow or creep rupture are of little or no concern. One exception to this is where the tension reinforcing might be limited to glass reinforcing. In this case if the sustained dead load on the tension reinforcing exceeds 25% of the ultimate strain of the laminate, then creep rupture may be a more valid concern. In cases where glass has been used as the primary tension reinforcing this criteria has been evaluated carefully in the design.

NCHRP also includes a short list of Non-Destructive Evaluation (NDE) techniques for evaluation of the laminate and the HCB in general. These test methods include the following:

- *Visual inspection and testing*
- *Tap testing*
- *Thermal testing*
- *Acoustic testing*
- *Ultrasonic testing*
- *Radiography*
- *Modal-parameter analysis*

Bridge B0439

HCB-Maintenance Manual

August 2012

As noted in the NCHRP report, all but the visual inspection and the tap test can be fairly costly or complicated methods. For many of the laminate damage types noted above, these two techniques may be more than adequate most of the time. However, the FRP laminate is only one component of the HCB. The other critical components include the arch concrete and the steel tension reinforcing. Like a concrete beam, the steel reinforcing in the HCB is not visible to the naked eye. As a result, there is always some concern about the condition evaluation of this component. Likewise, the concrete arch is not visible either. Neither the tap test nor visual inspection provides much guidance in condition evaluation of these two components. For the most part, the simple visual and tap test techniques should be sufficient for routine biennial inspections. It is recommended that at the end of ten years of service life, one of the more sophisticated NDE techniques be employed to determine if there is any deterioration or damage to the internal components of the HCB.

Another NDE technique that is becoming more common in the construction industry is "Ground Penetrating Radar" (GPR). This type of technology is used for a multitude of purposes, including location and condition evaluation of reinforcing steel and post-tensioning tendons as well as location of voids in post-tensioning grout. It is also becoming more popular as a technique for finding voids in concrete and condition evaluation of concrete. Although still more expensive than visual inspection and tap testing, this technology is becoming more readily available and may be warranted for a more thorough investigation than would be conducted under a normal biennial inspection.

It should be noted that the tension steel is protected by several barriers including; no less than 1/4" of high quality FRP laminate, complete encasement in the same vinyl ester resin as the laminate and a galvanized coating. Further, as noted before, the quantity of steel is typically on the order of twice that required for ultimate bending capacity. Likewise, the concrete arch is almost always in compression and is completely encapsulated. With proper placement of the concrete during construction, it is not likely that there will be any degradation of this component under normal service operations.

5.2 DETERMINATION OF RATING FOR HCB

As stated before, due to the newness of the HCB structures and the anticipated durability of the materials, there is no statistical database of damage or deterioration for assessing the condition rating of this portion of the bridge superstructure. Regardless, it is important to provide the inspector with some type of guidance in assessing the condition of the HCB to determine a consistent rating as is done with other types of bridge subcomponents. The following is to serve as a guideline to the inspector with respect to determination of the condition rating consistent with a scale ranging from 0 to 9. It should be noted that the current condition rating is purely based on the current understanding of the performance of the HCB and the FRP materials comprising the beams. It is also based on speculation of what types of damage and or degradation might result over time and how these might relate to similar ratings for other types of materials used in bridge superstructures. The inspector should exercise the proper standard of care in the assessment of the condition ratings and be cognizant of the likelihood that over time these condition assessments may need to be calibrated based on observed performance of the HCB.

Rating 9: Excellent Condition.

- A. No deficiencies noted.

Rating 8: Very Good Condition. *Potential exists for minor preventive maintenance.*

- A. No noticeable or noteworthy deficiencies that affect the condition of the superstructure.
- B. Insignificant cosmetic blemishes.

Rating 7: Good Condition. *Potential exists for minor maintenance.*

- A. Minor cracking in laminate matrix evident in the surface either from UV exposure, weather related damage or impact.
- B. Abrasion or scratches on the surface of the laminate, but do not penetrate the fibers.
- C. Small holes in the laminate due to impact or vandalism (e.g. bullet holes).
- D. Blistering or noticeable bubbles on the surface or gelcoat where applied.
- E. Minor concrete cracking in the cast-in-place diaphragms at piers and/or abutments.

Rating 6: Satisfactory Condition: *Potential exists for major maintenance.*

- A. Cracking and/or damage to the laminate with no evidence of damage or deterioration of the steel strands in the tension reinforcement.
- B. Abnormal undulations or mounds seen on the otherwise flat surface of the FRP surfaces on the HCB.

Bridge B0439

HCB-Maintenance Manual

August 2012

- C. The presence of moisture stains on the underside, away from the deck interface with no visible path for water collection. This could be a sign of porosity in the laminate.
- D. Heavy leaching through concrete diaphragms at girder encasement of integral bents.

Rating 5: Fair Condition: *Potential exists for minor rehabilitation.* No affect on structural capacity.

- A. Significant delamination of FRP from foam core.
- B. Exposure of steel tension reinforcement or concrete compression reinforcement through the laminate.
- C. Abrasion or scratches in the FRP laminate resulting in exposure of or severing of glass fibers.
- D. Collision or impact damage to FRP laminates.
- E. Considerable open cracking of concrete diaphragms at girder encasement of integral bents.
- F. Evidence of tearing of the FRP laminate along surfaces or at corners.

Rating 4: Poor Condition: *Potential exists for major rehabilitation.* Some affect on load capacity. Blocking or shoring may be required as precautionary measure.

- A. Evidence of rust or significant exposure of the steel tension reinforcement.
- B. Evidence of significant deterioration or crushing of the concrete compression reinforcement.
- C. Collision or impact damage resulting in large tears or penetrations of the FRP laminate, severing of tension or compression reinforcement, or any visibly evident significant distortions in the geometry of the HCB shell.
- D. Rust or spalling of concrete at the anchorage zones of the beam or in the concrete diaphragms at girder encasement of integral bents.
- E. Section loss of the laminate due to exposure to fire.

Rating 3: Serious Condition: *Repair or rehabilitation required immediately.*

- A. Any condition described in Rating 4, which is of a severe magnitude or for which blocking, shoring or load restrictions are necessary.
- B. Excessive deflections evident in the beams.

Rating 2: Critical Condition: CRITICAL INSPECTION FINDING. The need for repair or rehabilitation is urgent. Facility should be closed until the indicated repair is completed.

- A. Structure on verge of collapse or portion of superstructure has failed.

Rating 1: "Imminent" Failure Condition – facility is closed. CRITICAL INSPECTION FINDING. *Study should determine feasibility for repair. Corrective action may put structure back into light service.*

Rating 0: Failed Condition – facility is closed and beyond repair. *Replacement of structure is necessary.*

Again, the rating determinations shown above most likely will evolve over time as historical data related to the service performance of HCB bridges is documented. These suggested rating determinations are intended to be for the HCB component of the superstructure only. Other components of the bridge should be evaluated based on the criteria established in the *Critical Inspection Findings Missouri Bridge and Culvert Rating Guidelines*.

5.3 STRUCTURAL HEALTH MONITORING

One of the NDE methods listed in Report 564 also warrants further discussion not only for periodic inspections, but also for real time evaluation of the bridge. Currently there are a number of companies and universities focused on modal analysis of structures for damage assessment. Of the more sophisticated methods currently available, this technology seems to be benefitting from the evolution of consumer electronics. Many of these systems use simple accelerometers and wireless transmission technology to reduce the cost of instrumentation and data acquisition. Further, without having to know exactly where damage has occurred on a structure, these methods have the ability to triangulate off of an array of sensors and actually isolate location of damage that may not be evident from other means of investigation.

In general, these modal analysis techniques map a damage probability index based on acquiring a frequency response at some of the higher modes of vibration in an excited structure. In most cases the excitation can just be ambient traffic. It should be noted that a more accurate assessment of a structure results if there is a baseline measurement of the frequency response of the structure, e.g. if measurements are taken in a new bridge before any damage or degradation has occurred.

Bridge B0439

HCB-Maintenance Manual

August 2012

This technology is rapidly evolving and although no clear front-runner has evolved, this does appear to be a technology well suited to the HCB and other structures where critical structural components may not be visible.

5.4 REPAIRS

There are already well established methods for conventional repairs to prestressed concrete beams as well as steel beams, including localized patching of concrete and heat straightening of steel beams. Other methods that have recently evolved include bonding of carbon fibers to both concrete and steel girders for purposes both of repairing the girders as well as upgrading the capacities of these girders. It should be noted that the composite strengthening systems that have been developed have become rather common place and further lend themselves better to the repair of a composite laminate than they do concrete or steel. These FRP strengthening systems would be recommended for damage to the actual HCB shell.

Currently AASHTO is working towards Design Guide Specification for strengthening of concrete bridges using FRP laminates bonded to the existing structure. These technologies will, for the most part, parallel extensive work that has been done in ACI Committee 440 for the last two decades. The owner is encouraged to use these references for guidance in evaluating structural repairs to damaged HCB bridges.

It should be noted that the FRP strengthening criteria and methods developed for concrete sometimes require remediation to the concrete substrate prior to application. The same would be true for the HCB, although due to the completely different embodiment of the beam, the remediation measures will be different. In general, it is recommended that any unsuitable laminate be cut out of the structure. If there is damage to the foam core, the foam should be repaired and restored to the original geometry prior to bonding any new materials. If the foam is accessible, any damaged foam can be routed out. The surface can then be restored with simple spray in closed-cell expansive foams like "Great Stuff" that can be found at the local hardware store. If the repairs are extensive a specialty contractor and/or consultant should be contacted.

5.5 DECK REPLACEMENT

It is entirely likely that at some point during the life of the HCB Bridge, it will be necessary to replace the deck. In most applications the deck system on an HCB is no different from the reinforced concrete decks used on concrete or steel bridges. In fact the first HCB bridge ever constructed was a 30-foot railroad bridge constructed as part of the HSR-IDEA project. The only damage evident from the initial testing was cracking in the 4-inch concrete deck due to insufficient reinforcing. The deck on this bridge was subsequently removed and reconstructed a year later before resuming testing.

There are several precautions that should be taken in replacing the deck on an HCB Bridge. In most cases the HCB framing will have adequate capacity to support the removal equipment, however care should be taken in removal of the existing deck to make sure that the top flanges and more importantly the concrete fins above the arches are not damaged. It would be well advised to limit the size of the equipment allowed for removal of the deck concrete. It would also be preferable to use "chisel" type bits, instead of "pointed" bits to avoid penetrating the laminates. Although the laminates are very durable and can absorb tremendous amounts of energy, it is not impossible to penetrate.

If some damage is sustained to the laminate in the top flange, it should not compromise the structural capacity of the HCB. However prior to casting a new deck, the laminate should be repaired, as a minimum to make sure there are no openings that allow for ingress of water or other materials. Likewise, care should be taken not to damage the shear connectors extending out of the beam. Any damage to the galvanized coating on the shear connectors should be repaired prior to casting a new deck. It may be possible to drill in additional shear connectors, if damaged, but this is less than desirable.

Another consideration for deck replacement is that it may be more difficult to install protective shielding for removal of the existing deck. As the HCB typically does not have flanges extending out at the bottom, there is no simple location to attach the cribbing to support the shields. In some cases, the top flanges of the HCB are adjacent and no shielding is necessary. If it is a requirement, it may be necessary to attach some type of angle or appurtenance to support the shielding.

REPORT DOCUMENTATION PAGE

Form Approved
OMB No. 0704-0188

Public reporting burden for this collection of information is estimated to average 1 hour per response, including the time for reviewing instructions, searching existing data sources, gathering and maintaining the data needed, and completing and reviewing this collection of information. Send comments regarding this burden estimate or any other aspect of this collection of information, including suggestions for reducing this burden to Department of Defense, Washington Headquarters Services, Directorate for Information Operations and Reports (0704-0188), 1215 Jefferson Davis Highway, Suite 1204, Arlington, VA 22202-4302. Respondents should be aware that notwithstanding any other provision of law, no person shall be subject to any penalty for failing to comply with a collection of information if it does not display a currently valid OMB control number. **PLEASE DO NOT RETURN YOUR FORM TO THE ABOVE ADDRESS.**

1. REPORT DATE (DD-MM-YYYY) September 2016			2. REPORT TYPE Final Technical Report			3. DATES COVERED (From - To)		
4. TITLE AND SUBTITLE Demonstration of Corrosion-Resistant Hybrid Composite Bridge Beams for Structural Applications: Final Report on Project F12-AR15						5a. CONTRACT NUMBER		
						5b. GRANT NUMBER		
						5c. PROGRAM ELEMENT NUMBER Corrosion Prevention and Control		
6. AUTHOR(S) Chris Olaes, Steven C. Sweeney, Richard G. Lampo, James Wilcoski, and Larry Clark						5d. PROJECT NUMBER F12-AR15		
						5e. TASK NUMBER		
						5f. WORK UNIT NUMBER		
7. PERFORMING ORGANIZATION NAME(S) AND ADDRESS(ES) U.S. Army Engineer Research and Development Center Construction Engineering Research Laboratory 2902 Newmark Drive/P.O. Box 9005 Champaign, IL 61826-9005						8. PERFORMING ORGANIZATION REPORT NUMBER ERDC/CERL TR-16-22		
9. SPONSORING / MONITORING AGENCY NAME(S) AND ADDRESS(ES) Office of the Secretary of Defense (OUSD(AT&L)) 3090 Defense Pentagon Washington, DC 20301-3090						10. SPONSOR/MONITOR'S ACRONYM(S) OUSD(AT&L)		
						11. SPONSOR/MONITOR'S REPORT NUMBER(S)		
12. DISTRIBUTION / AVAILABILITY STATEMENT Approved for public release; distribution is unlimited.								
13. SUPPLEMENTARY NOTES								
14. ABSTRACT The Army has 1,500 vehicular bridges on its installations that can incur high maintenance costs and even early replacement as a result of corrosion of the steel support structures or the reinforcing bar in the concrete. The application of corrosion-resistant technology can extend the service life of bridges and reduce maintenance costs. The Office of the Secretary of Defense Corrosion Prevention and Control Program project demonstrated and validated a corrosion-resistant hybrid-composite beam (HCB) for the reconstruction of a one span of a traditional steel and concrete bridge at Fort Knox, Kentucky. The HCBs were installed on half of the bridge, and conventional steel beams were installed on the other half. Structural analysis of the bridge was performed, and the span with HCBs was found to meet all design specifications and load ratings. This technology can increase the life cycle of bridge infrastructure when utilized in new construction and replacement by the Army and all other federal agencies. The technology's return on investment (ROI) is 4.22.								
15. SUBJECT TERMS Structural dynamics; Bridges–Live loads; Bridges–Design and construction; Composite materials–Testing; Corrosion-resistant materials; Composite construction, Corrosion Prevention and Control (CPC) Program; Hybrid composite beam (HCB); Fort Knox, Kentucky								
16. SECURITY CLASSIFICATION OF:				17. LIMITATION OF ABSTRACT	18. NUMBER OF PAGES	19a. NAME OF RESPONSIBLE PERSON		
a. REPORT Unclassified	b. ABSTRACT Unclassified	c. THIS PAGE Unclassified		U/U	105	19b. TELEPHONE NUMBER (include area code)		